Bayesian Estimation of Macro-Finance DSGE Models with Stochastic Volatility

David E. Rapach*
Washington University in St. Louis and
Saint Louis University
david.rapach@wustl.edu

Fei Tan
Saint Louis University
fei.tan@slu.edu

March 17, 2020

*Corresponding author. Send correspondence to David E. Rapach, Department of Finance, Olin Business School, Washington University in St. Louis, St. Louis, MO 63130; email: david.rapach@wustl.edu; phone: 314-935-3318. We thank seminar and conference participants at the City University of Hong Kong, Cyprus University of Technology, Federal Reserve Bank of Atlanta, Indiana University, National University of Singapore, Saint Louis University, Singapore Management University, 2016 Midwest Econometrics Group Meeting, 2017 Computing in Economics and Finance Conference, 2017 NBER-NSF Seminar on Bayesian Inference and Econometrics, 2018 International Association of Applied Econometrics Conference, and 2019 Dynare Conference, as well as Yoosoon Chang, Siddhartha Chib, Bong-Geun Choi, and Minchul Shin, for very helpful comments. A MATLAB toolbox (DSGE-SV-affine) for implementing the Bayesian MCMC algorithm developed in this paper is available at https://sites.google.com/slu.edu/daverapach/dsge-sv-affine.

Bayesian Estimation of Macro-Finance DSGE Models with Stochastic Volatility

Abstract

We develop a Bayesian Markov chain Monte Carlo algorithm for estimating risk premia in dynamic stochastic general equilibrium (DSGE) models with stochastic volatility. Our approach is fully Bayesian and employs an affine solution strategy that makes estimation of large-scale DSGE models computationally feasible. We use our algorithm to estimate the US equity risk premium in a DSGE model that includes time-preference, technology, investment, and volatility shocks. Time-preference and technology shocks are primarily responsible for the sizable equity risk premium in the estimated DSGE model. The estimated historical stochastic volatility and equity risk premium series display pronounced countercyclical fluctuations.

JEL classifications: C11, C32, C58, E32, E44, G12

Keywords: Stochastic volatility, Affine solution, Gibbs sampler, Equity risk premium, Structural shocks, Business cycle

1 Introduction

Dynamic stochastic general equilibrium (DSGE) models allow for the identification of the "deep" structural shocks that ultimately determine risk premia, thereby illuminating the economic mechanisms by which the underlying structural shocks that generate business-cycle fluctuations affect equilibrium asset prices. Indeed, building on the early studies of Rouwenhorst (1995), Jermann (1998), Lettau and Uhlig (2000), Tallarini (2000), Boldrin et al. (2001), and Lettau (2003), researchers are increasingly turning to DSGE models to analyze risk premia.[1] On a largely parallel track, DSGE models are increasingly incorporating stochastic volatility.[2] Reduced-form models in empirical asset pricing also often include stochastic volatility.[3] In this paper, we merge these lines of the literature by developing a Bayesian approach for estimating risk premia in DSGE models with stochastic volatility.

Our approach has three key features. First, it is *fully Bayesian*: we simulate draws from the joint posterior distribution for both the model parameters and latent stochastic volatility series. Second, by employing an *affine solution* based on log-normality (Jermann 1998; Lettau 2003; Dew-Becker 2012; Malkhozov 2014), we estimate risk premia in a manner that substantially reduces computational costs, so that our approach can be used to estimate risk premia in large-scale DSGE models with stochastic volatility. Third, since stochastic volatility appears as an additional state variable in the affine solution, we permit *non-zero responses to volatility shocks*.

Existing Bayesian methods offer some of these features, but not all three simultaneously. Fernández-Villaverde and Rubio-Ramírez (2007) rely on a second-order perturbation approximation to the solution and particle filtering to make likelihood-based inferences in DSGE

[1] See, for example, Guvenen (2009), Ai (2010), Kaltenbrunner and Lochstoer (2010), Andreasen (2012), van Binsbergen et al. (2012), Gourio (2012), Rudebusch and Swanson (2012), Ai et al. (2013), Croce (2014), Dew-Becker (2014), Li and Palomino (2014), Hirshleifer et al. (2015), Kung (2015), Chen (2016), Favilukis and Lin (2016), Chen (2017), Kilic and Wachter (2018), and Croce et al. (2019).

[2] See, for example, Fernández-Villaverde and Rubio-Ramírez (2007), Justiniano and Primiceri (2008), Bloom (2009), Fernández-Villaverde et al. (2011, 2015a,b), and Diebold et al. (2017).

[3] See, for example, Bansal and Yaron (2004), Bansal et al. (2012, 2016), Beeler and Campbell (2012), Hasseltoft (2012), Bansal and Shaliastovich (2013), Albuquerque et al. (2016), and Nakamura et al. (2017).

models. While their approach allows for risk premia in the model solution, it is not fully Bayesian and does not permit non-zero responses to volatility shocks. Justiniano and Primiceri (2008) develop a fully Bayesian approach for estimating DSGE models with stochastic volatility; however, they use a conventional log-linearized approximation that precludes risk premia and non-zero responses to volatility shocks. Fernández-Villaverde et al. (2015b) refine the particle-filtering approach of Fernández-Villaverde and Rubio-Ramírez (2007), but their approach is still not fully Bayesian and does not allow non-zero responses to volatility shocks. Like Justiniano and Primiceri (2008), Diebold et al. (2017) employ a fully Bayesian procedure that precludes risk premia and non-zero responses to volatility shocks.[4]

The conventional perturbation solution relies on a log-linearized approximation and thus entails certainty equivalence, so that higher-order approximations are required to compute risk premia. Furthermore, a third-order perturbation approximation is needed for non-zero responses to volatility shocks (Fernández-Villaverde et al. 2011; Caldara et al. 2012),[5] while a sixth-order perturbation approximation is required for the "volatility of volatility" parameter of the stochastic volatility process to appear in the DSGE model solution (de Groot 2015, 2016). Such higher-order solutions (as well as projection methods) quickly encounter the curse of dimensionality, which renders them infeasible for likelihood-based estimation of large-scale DSGE models with stochastic volatility. In contrast, the affine solution includes risk premia, permits non-zero responses to volatility shocks, and contains the volatility of volatility parameter in the model solution, all while avoiding the curse of dimensionality. Presently, even to include second-order terms in Bayesian estimation of DSGE models with stochastic volatility, a researcher needs to turn to the approach of Fernández-Villaverde et al. (2015b), which is not fully Bayesian and does not allow for non-zero responses to volatility shocks (and does not include the volatility of volatility parameter in the solution).

[4]With respect to non-likelihood-based approaches, Andreasen (2012) and Croce (2014) analyze risk premia in DSGE models with stochastic volatility via calibration, while Born and Pfeifer (2014) estimate a DSGE model with stochastic volatility using a two-step procedure based on particle filtering and simulated method of moments.

[5]Benigno et al. (2013) modify the Schmitt-Grohé and Uribe (2004) perturbation approach to permit non-zero responses to volatility shocks in a second-order approximation to the solution.

We use the *level* instead of *log* specification for stochastic volatility. We do so for three primary reasons. First, in exploiting log-normality, the level of stochastic volatility naturally arises as an additional state variable in the affine model solution; in conjunction with the law of motion for stochastic volatility, we can thus solve the model directly in terms of the level of stochastic volatility. Second, Andreasen (2010) argues that log stochastic volatility coupled with log model variables imply unbounded conditional and unconditional moments for the levels of model variables; because our approach involves log-linearization, the argument applies to our case. Third, the level specification for stochastic volatility is more in line with the convention in the finance literature (e.g., Bansal and Yaron 2004).

Existing Bayesian methods for estimating stochastic volatility processes rely on the log specification (e.g., Kim et al. 1998). We thus develop a Markov chain Monte Carlo (MCMC) algorithm for sampling from the joint posterior distribution for the parameters and latent stochastic volatility levels of a stochastic volatility process. The MCMC algorithm is based on Gibbs sampling with data augmentation (Tanner and Wong 1987), as well as the tailoring of proposal densities for Metropolis-Hastings (MH) steps (Chib and Greenberg 1994, 1995).

We incorporate our procedure for estimating a stochastic volatility process in levels into a larger MCMC algorithm to develop a framework for estimating risk premia in DSGE models with stochastic volatility. The larger algorithm has two primary Gibbs steps. In the first step, we use the affine solution, a conditional version of the Kalman filter, and the Chib and Ramamurthy (2010) tailored randomized block MH (TaRB-MH) algorithm to draw the DSGE model parameters conditional on the stochastic volatility series and the data. The second step of the Gibbs sampler entails data augmentation, and we use a suitably modified version of our proposed Bayesian procedure to draw the elements of the stochastic volatility series conditional on the DSGE model parameters and the data.

We apply our MCMC algorithm to estimate the US equity risk premium in a DSGE model with recursive preferences and stochastic volatility. In addition to volatility shocks, the DSGE model includes time-preference and technology shocks, as well as shocks to capital

adjustment costs (i.e., investment shocks). Using quarterly data for 1973 to 2018 for five observable variables, we obtain plausible estimates of 1.79 and 10.30 for the elasticity of intertemporal substitution (EIS) and coefficient of relative risk aversion (RRA), respectively.

From a structural perspective, we find that time-preference and technology shocks play leading roles in generating a large steady-state equity risk premium in the estimated DSGE model. The importance of the former accords with Albuquerque et al. (2016), who find that time-preference shocks—by creating what they call "valuation risk"—are the principal source of the equity risk premium in an endowment economy framework. The relevance of technology shocks aligns with Kaltenbrunner and Lochstoer (2010), who show how such shocks endogenously generate long-run risk (Bansal and Yaron 2004) in a production economy. More directly in terms of asset pricing, time-preference and technology shocks generate strong negative covariation between equity return and stochastic discount factor (SDF) innovations, thereby contributing to a large equity risk premium. In contrast, investment and volatility shocks generate positive covariation between equity return and SDF innovations, so that these shocks contribute to a negative equity risk premium; however, their joint contribution is limited relative to that of time-preference and technology shocks, so that on net the estimated DSGE model delivers a large steady-state equity risk premium.

The estimated historical stochastic volatility series in the DSGE model evinces pronounced countercyclical fluctuations, which translate into corresponding fluctuations in the estimated historical equity risk premium. Such countercyclical fluctuations in the equity risk premium concur with empirical results from predictive regressions (e.g., Fama and French 1989; Cooper and Priestly 2009; Rapach et al. 2010). The magnitudes of the fluctuations in the estimated historical equity risk premium are economically significant: the annualized equity risk premium typically rises by approximately 600 basis points from just prior to a business-cycle peak to just after a trough.

The rest of the paper is organized as follows. Section 2 discusses the affine solution method. Section 3 describes our MCMC algorithm for estimating a stochastic volatility

process in levels. Section 4 presents the larger MCMC algorithm for estimating DSGE models with stochastic volatility. Section 5 specifies the DSGE model. Section 6 reports the estimation results, while Section 7 explores the determinants of the equity risk premia. Section 8 concludes.

2 Affine Solution

In the spirit of Jermann (1998) and Lettau (2003), Dew-Becker (2012) and Malkhozov (2014) propose affine solution procedures based on log-normality. Because it substantially reduces computational costs, while still capturing important aspects of the model solution, an affine solution is a key component of our approach for estimating risk premia in DSGE models with stochastic volatility.

Consider a dynamic system for the vector of model variables, $\mathbf{x}_t$, which are comprised of endogenous variables and exogenous shocks. Following standard practice, we assume that the exogenous shocks follow autoregressive (AR) processes. The AR processes are driven by a vector of innovations, $\boldsymbol{\varepsilon}_{t+1} \sim \mathcal{N}(\mathbf{0}, \boldsymbol{\Sigma})$, where $\mathbf{0}$ is a suitably sized vector of zeros and $\boldsymbol{\Sigma}$ is diagonal. We divide the system into three types of equations. The first consists of Euler equations involving conditional expectations:

$$E_t[F(\mathbf{x}_{t+1}, \mathbf{x}_t)] = \mathbf{1}, \tag{2.1}$$

where $E_t(\cdot)$ is the expectations operator conditional on information available through period t and $\mathbf{1}$ is a suitably sized vector of ones. The second type is comprised of non-expectational equations (e.g., budget constraints and production functions), which we approximate via log-linearization in the usual manner. The third type is the aforementioned AR processes for the exogenous shocks.

Let $D(\mathbf{x}_{t+1}, \mathbf{x}_t) = \log[F(\mathbf{x}_{t+1}, \mathbf{x}_t)]$ and $\hat{\mathbf{x}}_t = \log(\mathbf{x}_t) - \log(\bar{\mathbf{x}})$, where $\bar{\mathbf{x}}$ is the vector of non-stochastic steady-state values for $\mathbf{x}_t$. Note that $\exp\big(\bar{D}\big) = \mathbf{1}$ in the non-stochastic steady

state, where $\bar{D} = \log[F(\bar{\mathbf{x}}, \bar{\mathbf{x}})]$. We approximate Equation (2.1) using

$$\log\{E_t[\exp(\mathbf{D}_+\hat{\mathbf{x}}_{t+1} + \mathbf{D}_0\hat{\mathbf{x}}_t)]\} = \mathbf{0}, \tag{2.2}$$

where

$$\mathbf{D}_+ = \frac{\partial D(\exp[\log(\bar{\mathbf{x}})], \exp[\log(\bar{\mathbf{x}})])}{\partial \log(\mathbf{x}_{t+1})} = \frac{\partial D(\bar{\mathbf{x}}, \bar{\mathbf{x}})}{\partial \mathbf{x}_{t+1}} \text{diag}(\bar{\mathbf{x}}), \tag{2.3}$$

$$\mathbf{D}_0 = \frac{\partial D(\exp[\log(\bar{\mathbf{x}})], \exp[\log(\bar{\mathbf{x}})])}{\partial \log(\mathbf{x}_t)} = \frac{\partial D(\bar{\mathbf{x}}, \bar{\mathbf{x}})}{\partial \mathbf{x}_t} \text{diag}(\bar{\mathbf{x}}), \tag{2.4}$$

and $\text{diag}(\bar{\mathbf{x}})$ is a suitably sized diagonal matrix with the vector $\bar{\mathbf{x}}$ along its main diagonal. Suppose that the model solution takes an affine form:

$$\hat{\mathbf{x}}_t = \mathbf{c} + \mathbf{G}\hat{\mathbf{x}}_{t-1} + \mathbf{M}\boldsymbol{\varepsilon}_t, \tag{2.5}$$

where the elements of $\mathbf{c}$, $\mathbf{G}$, and $\mathbf{M}$ are functions of the DSGE model parameters. The constant term $\mathbf{c}$ in Equation (2.5) accounts for the *risk adjustment* to the solution. Conventional log-linearized approximations of the Euler equations entail certainty equivalence and thus neglect the risk adjustment. Using Equation (2.5) and the property of log-normally distributed random variables, we can evaluate Equation (2.2) as

$$\mathbf{D}_+E_t(\hat{\mathbf{x}}_{t+1}) + \mathbf{D}_0\hat{\mathbf{x}}_t + 0.5\,\text{diag}\big(\mathbf{D}_+\mathbf{M}\boldsymbol{\Sigma}\mathbf{M}'\mathbf{D}_+'\big) = \mathbf{0}, \tag{2.6}$$

where the last term on the left-hand side is a risk adjustment; again, conventional log-linearized approximations ignore this term and thus preclude the appearance of risk premia in the solution.

In conjunction with the AR processes for the exogenous shocks and usual log-linearized approximations of the non-Euler equations, Equation (2.6) constitutes an affine system of expectational difference equations in the model variables. Because the system depends on the

as-yet-unknown matrix $\mathbf{M}$, we can obtain the affine solution in Equation (2.5) by following Malkhozov (2014) and using a "guess-and-verify" method for small models or Dew-Becker (2012) by using an iterative procedure based on the Gensys program (Sims 2002) for high-dimensional models. For the latter case, in practice, only two iterations of Gensys are needed—one without and one with the risk-adjustment term in Equation (2.6)—as $\mathbf{G}$ and $\mathbf{M}$ are independent of $\mathbf{c}$ in Equation (2.5).[6]

Next, we introduce stochastic volatility. Analogously to Bansal and Yaron (2004), we assume that a common stochastic volatility component σ_t^2 underlies time-varying volatility,[7] so that $\boldsymbol{\varepsilon}_{t+1} \sim \mathcal{N}(\mathbf{0}, \mathbf{H}\sigma_t^2)$, where $\mathbf{H}$ is a diagonal matrix with non-negative elements and σ_t^2 evolves according to a stationary AR process:

$$\sigma_{t+1}^2 = (1-\rho_\sigma)\sigma^2 + \rho_\sigma \sigma_t^2 + \underbrace{\varphi_\sigma e_{\sigma,t+1}}_{\varepsilon_{\sigma,t+1}}, \tag{2.7}$$

where $\sigma \geq 0$ is the steady-state level of volatility, $0 \leq \rho_\sigma < 1$, $\varphi_\sigma \geq 0$, and $e_{\sigma,t+1} \sim$ i.i.d. $\mathcal{N}(0,1)$. We extend the vectors of model variables and innovations to

$$\mathbf{s}_t = [\ \hat{\mathbf{x}}_t' \quad \sigma_t^2\ ]', \tag{2.8}$$

$$\boldsymbol{\omega}_{t+1} = [\ \boldsymbol{\varepsilon}_{t+1}' \quad \varepsilon_{\sigma,t+1}\ ]' \sim \mathcal{N}(\mathbf{0}, \boldsymbol{\Sigma}_t), \tag{2.9}$$

respectively, where

$$\boldsymbol{\Sigma}_t = \begin{bmatrix} \mathbf{H}\sigma_t^2 & \mathbf{0} \\ \mathbf{0}' & \varphi_\sigma^2 \end{bmatrix}. \tag{2.10}$$

Replacing $\hat{\mathbf{x}}_t$, $\boldsymbol{\varepsilon}_t$, and $\boldsymbol{\Sigma}$ with $\mathbf{s}_t$, $\boldsymbol{\omega}_t$, and $\boldsymbol{\Sigma}_t$, respectively, in Equations (2.5) and (2.6), it is straightforward to see that the system of expectational difference equations is still affine in

[6]The Internet Appendix compares the second-order perturbation and affine solutions for the simple neoclassical growth model in Schmitt-Grohé and Uribe (2004). The constant (i.e., risk-adjustment) and first-order terms are approximately equal for the two solutions.

[7]In an endowment economy framework, Bansal and Yaron (2004) specify a common volatility component for the innovations to reduced-form consumption and dividend growth processes.

the model variables, $\mathbf{s}_t$. We can thus compute the risk-adjusted solution using the iterative procedure based on Gensys.[8]

In the standard perturbation approach, a first-order solution approximation neglects all model dynamics induced by stochastic volatility (due to certainty equivalence), while a second-order approximation captures the volatility effect only through the primitive shocks (i.e., the *indirect* role). As shown by Fernández-Villaverde et al. (2011), it is only through a third-order perturbation approximation to the solution that the responses of the variables of interest to volatility shocks can generally be non-zero (i.e., the *direct* role). By not approximating the primitive shocks, Benigno et al. (2013) develop a modified second-order perturbation method that retains both indirect and direct roles for volatility shocks, whereas the affine solution retains both roles by exploiting the property of log-normality.[9]

In summary, the affine solution based on log-normality includes risk premia and permits non-zero responses of variables of interest to volatility shocks.[10] At the same time, it allows us to circumvent the curse of dimensionality that makes higher-order perturbation approximations and projection methods practically infeasible in our context. Of course, this comes at the cost of neglecting higher-order terms; in many instances, such higher-order terms are quantitatively small. In general, whether it is appropriate to ignore higher-order terms involves consideration of the tradeoffs involved in implementing likelihood-based estimation.

3 MCMC Algorithm for Stochastic Volatility

To fix ideas, consider a simple reduced-form model for y_t with stochastic volatility:

$$y_t = \alpha + \varepsilon_{y,t}, \tag{3.1}$$

[8]More than two iterations of the Gensys program are typically needed to compute the solution for DSGE models with stochastic volatility. The affine solution (as well as the Bayesian MCMC algorithm in Section 4) can be suitably modified to accommodate separate stochastic volatility processes for each shock.

[9]The Internet Appendix compares the Benigno et al. (2013) second-order perturbation and affine solutions for the simple neoclassical growth model in Schmitt-Grohé and Uribe (2004) when the model is characterized by stochastic volatility. The two solutions are very similar.

[10]The volatility of volatility parameter (φ_σ) also appears in the affine solution.

where $\varepsilon_{y,t} \sim \mathcal{N}(0, \sigma_t^2)$ and σ_t^2 follows the AR process in Equation (2.7). We simulate posterior draws for the model parameters and stochastic volatility series using an MCMC algorithm based on Gibbs sampling with data augmentation. Defining $\mathbf{y} = [\ y_1 \quad \cdots \quad y_T\ ]'$ and $\boldsymbol{\sigma}^2 = \{\sigma_t^2\}_{t=1}^T$, the Gibbs sampler has two primary steps:

(1) Draw $(\alpha, \sigma, \rho_\sigma, \varphi_\sigma)$ given $(\mathbf{y}, \boldsymbol{\sigma}^2)$.

(2) Draw $\boldsymbol{\sigma}^2$ given $(\mathbf{y}, \alpha, \sigma, \rho_\sigma, \varphi_\sigma)$.

Using Equations (2.7) and (3.1) and applying Bayes' theorem, we can express the posterior kernel density for the first Gibbs step as

$$p(\alpha, \sigma, \rho_\sigma, \varphi_\sigma | \mathbf{y}, \boldsymbol{\sigma}^2) \propto \left[\prod_{t=1}^T p_{\mathcal{N}}\big(y_t | \alpha, \sigma_t^2\big)\right]\left[\prod_{t=1}^T p_{\mathcal{N}}\big(\sigma_t^2 | (1-\rho_\sigma)\sigma^2 + \rho_\sigma \sigma_{t-1}^2, \varphi_\sigma^2\big)\right] p(\alpha, \sigma, \rho_\sigma, \varphi_\sigma), \tag{3.2}$$

where $p(\alpha, \sigma, \rho_\sigma, \varphi_\sigma)$ is the joint prior density for the parameters and $p_{\mathcal{N}}(\cdot|a, b)$ denotes the normal density with mean a and variance b. Following convention, we treat the joint prior density as the product of independent marginal prior densities:

$$p(\alpha, \sigma, \rho_\sigma, \varphi_\sigma) = p(\alpha)p(\sigma)p(\rho_\sigma)p(\varphi_\sigma). \tag{3.3}$$

The posterior kernel density in Equation (3.2) is not from a known family of distributions, so that we use the MH algorithm to simulate draws. A key aspect of our procedure is the tailoring of proposal densities for the MH algorithm, which substantially enhances sampling efficiency. We use a multivariate student's t distribution with ten degrees of freedom as the proposal density, and we tailor the proposal density by centering (scaling) it using the numerically computed mode (inverse of the negative of the Hessian) in Equation (3.2).[11]

Turning to the second (data-augmentation) step in the Gibbs sampler, we simulate draws from $p\big(\boldsymbol{\sigma}^2 \big| \mathbf{y}, \alpha, \sigma, \rho_\sigma, \varphi_\sigma\big)$ via Gibbs sampling by alternately drawing from

[11] We use the `MATLAB` function `csminwel.m` (available from Christopher Sims's webpage at `http://www.princeton.edu/~sims/`) to numerically compute the mode and Hessian for the log posterior kernel density.

$p\big(\sigma_t^2\big|\boldsymbol{\sigma}_{\setminus t}^2, \mathbf{y}, \alpha, \sigma, \rho_\sigma, \varphi_\sigma\big)$ for $t = 1, \ldots, T$, where

$$\boldsymbol{\sigma}_{\setminus t}^2 = \big\{\sigma_1^2, \ldots, \sigma_{t-1}^2, \sigma_{t+1}^2, \ldots, \sigma_T^2\big\}. \tag{3.4}$$

Using Equations (2.7) and (3.1), applying Bayes's theorem, and ignoring terms not involving σ_t^2, we can write the posterior kernel density as

$$\begin{aligned} p\big(\sigma_t^2\big|\boldsymbol{\sigma}_{\setminus t}^2, \mathbf{y}, \alpha, \sigma, \rho_\sigma, \varphi_\sigma\big) \propto p_{\mathcal{N}}\big(y_t\big|\alpha, \sigma_t^2\big) p_{\mathcal{N}}\big(\sigma_{t+1}^2\big|(1-\rho_\sigma)\sigma^2 + \rho_\sigma\sigma_t^2, \varphi_\sigma^2\big) \cdots \\ p_{\mathcal{N}}\big(\sigma_t^2\big|(1-\rho_\sigma)\sigma^2 + \rho_\sigma\sigma_{t-1}^2, \varphi_\sigma^2\big). \end{aligned} \tag{3.5}$$

We use the following procedure to draw σ_t^2 for $t = 1, \ldots, T$ from Equation (3.5) for a sweep of the Gibbs sampler:

(1) **Initialization** Set $\sigma_0^2 = \sigma^2$.

(2) **Recursion** For $t = 1, \ldots, T-1$, compute the posterior kernel density for σ_t^2 in Equation (3.5) and sample σ_t^2 using the MH algorithm with a tailored proposal density.

(3) **Terminal Condition** For $t = T$, Equation (3.5) becomes

$$p\big(\sigma_T^2\big|\boldsymbol{\sigma}_{\setminus T}^2, \mathbf{y}, \alpha, \sigma, \rho_\sigma, \varphi_\sigma\big) \propto p_{\mathcal{N}}\big(y_T\big|\alpha, \sigma_T^2\big) p_{\mathcal{N}}\big(\sigma_T^2\big|(1-\rho_\sigma)\sigma^2 + \rho_\sigma\sigma_{T-1}^2, \varphi_\sigma^2\big). \tag{3.6}$$

We compute the posterior kernel density for σ_T^2 in Equation (3.6) and again sample σ_T^2 using the MH algorithm with a tailored proposal density.

A univariate student's t distribution with ten degrees of freedom serves as the proposal density for Equations (3.5) and (3.6). Because we use the level (instead of log) specification for stochastic volatility, we need to restrict the σ_t^2 draws to be non-negative.[12]

We demonstrate the sampling efficiency of our procedure by estimating Equations (2.7) and (3.1) for the US log equity market excess return, where we generate 11,000 draws via

[12]Negative σ_t^2 draws from the tailored proposal density are very rare in our applications. When they do occur, we prevent a negative volatility draw by setting the MH acceptance probability to zero.

the MCMC algorithm and discard the first 1,000 burn-in draws. The complete results are available in the Internet Appendix; they indicate that the Markov chain mixes well.

4 MCMC Algorithm for DSGE Models

Analogously to Section 3, we employ an MCMC algorithm based on Gibbs sampling with MH steps and data augmentation to simulate posterior draws for the vector of DSGE model parameters (denoted by $\boldsymbol{\theta}$) and stochastic volatility series. Defining $\mathbf{Y} = [\ \mathbf{y}_1 \ \cdots \ \mathbf{y}_T\ ]'$, where $\mathbf{y}_t$ is the vector of observable variables for period t, the algorithm proceeds by alternately drawing from the following conditional posterior densities in two primary Gibbs steps:

(1) Draw $\boldsymbol{\theta}$ given $(\mathbf{Y}, \boldsymbol{\sigma}^2)$.

(2) Draw $\boldsymbol{\sigma}^2$ given $(\mathbf{Y}, \boldsymbol{\theta})$.

4.1 First Gibbs Step

Based on Bayes' theorem,

$$p\big(\boldsymbol{\theta}|\mathbf{Y}, \boldsymbol{\sigma}^2\big) \propto p\big(\mathbf{Y}|\boldsymbol{\theta}, \boldsymbol{\sigma}^2\big)p\big(\boldsymbol{\sigma}^2\big|\boldsymbol{\theta}\big)p(\boldsymbol{\theta}), \tag{4.1}$$

where $p(\boldsymbol{\theta})$ is the prior density for the DSGE model parameters; again, following convention, the joint prior density $p(\boldsymbol{\theta})$ is the product of independent marginal densities for the individual elements of $\boldsymbol{\theta}$. Let $\boldsymbol{\theta}^{(j)}$ and $\boldsymbol{\sigma}^{2,(j)}$ denote entities for the jth sweep of the MCMC algorithm. For a given sweep, we first draw $\boldsymbol{\theta}$ from Equation (4.1) using the Chib and Ramamurthy (2010) TaRB-MH procedure. The procedure begins by randomly generating blocks of the parameters $(\boldsymbol{\theta}_1, \ldots, \boldsymbol{\theta}_b)$. For each block $\boldsymbol{\theta}_k$ $(k = 1, \ldots, b)$, we draw $\boldsymbol{\theta}_k$ via an MH step with a tailored proposal density. Letting $\boldsymbol{\theta}^{(j)}_{k_1:k_2}$ denote blocks k_1 through k_2 for the jth sweep, the mean vector for the tailored proposal density is given by

$$\hat{\boldsymbol{\theta}}^{(j)}_k = \underset{\boldsymbol{\theta}^{(j)}_k}{\arg\max} \log\Big[p\Big(\mathbf{Y}\big|\boldsymbol{\theta}^{(j)}_{1:k-1}, \boldsymbol{\theta}^{(j)}_k, \boldsymbol{\theta}^{(j-1)}_{k+1:b}, \boldsymbol{\sigma}^{2,(j-1)}\Big)p\Big(\boldsymbol{\sigma}^{2,(j-1)}\big|\boldsymbol{\theta}^{(j)}_{1:k-1}, \boldsymbol{\theta}^{(j)}_k, \boldsymbol{\theta}^{(j-1)}_{k+1:b}\Big)p\Big(\boldsymbol{\theta}^{(j)}_k\Big)\Big], \tag{4.2}$$

while its scaling matrix is given by

$$\hat{\boldsymbol{\Sigma}}_k^{(j)} = \left\{ -\frac{\partial^2 \log\Big[p\Big(\mathbf{Y}|\boldsymbol{\theta}_{1:k-1}^{(j)}, \boldsymbol{\theta}_k^{(j)}, \boldsymbol{\theta}_{k+1:b}^{(j-1)}, \boldsymbol{\sigma}^{2,(j-1)}\Big) p\Big(\boldsymbol{\sigma}^{2,(j-1)}|\boldsymbol{\theta}_{1:k-1}^{(j)}, \boldsymbol{\theta}_k^{(j)}, \boldsymbol{\theta}_{k+1:b}^{(j-1)}\Big) p\Big(\boldsymbol{\theta}_k^{(j)}\Big)\Big]}{\partial \boldsymbol{\theta}_k^{(j)} \boldsymbol{\theta}_k^{(j)\prime}} \right\}^{-1} \tag{4.3}$$

evaluated at $\boldsymbol{\theta}_k^{(j)} = \hat{\boldsymbol{\theta}}_k^{(j)}$. As in Section 3, we use a multivariate student's t density with ten degrees of freedom as the proposal density. Proceeding through the b blocks, we generate the vector of DSGE model parameter draws for the jth sweep:

$$\boldsymbol{\theta}^{(j)} = [\ \boldsymbol{\theta}_1^{(j)\prime} \quad \cdots \quad \boldsymbol{\theta}_b^{(j)\prime}\ ]'. \tag{4.4}$$

To compute the value of the likelihood function $p(\mathbf{Y}|\boldsymbol{\theta}, \boldsymbol{\sigma}^2)$ in Equations (4.1) to (4.3), we use a conditional version of the Kalman filter, where we condition on $\boldsymbol{\sigma}^2$. We can express Equation (2.5) as

$$\underbrace{\begin{bmatrix} \hat{\mathbf{x}}_t \\ \sigma_t^2 \end{bmatrix}}_{\mathbf{s}_t} = \underbrace{\begin{bmatrix} \mathbf{c}_1 \\ c_2 \end{bmatrix}}_{\mathbf{c}} + \underbrace{\begin{bmatrix} \mathbf{G}_{11} & \mathbf{G}_{12} \\ 0 & \rho_\sigma \end{bmatrix}}_{\mathbf{G}} \underbrace{\begin{bmatrix} \hat{\mathbf{x}}_{t-1} \\ \sigma_{t-1}^2 \end{bmatrix}}_{\mathbf{s}_{t-1}} + \underbrace{\begin{bmatrix} \mathbf{M}_{11} & \mathbf{M}_{12} \\ 0 & 1 \end{bmatrix}}_{\mathbf{M}} \underbrace{\begin{bmatrix} \boldsymbol{\varepsilon}_t \\ \varepsilon_{\sigma,t} \end{bmatrix}}_{\boldsymbol{\omega}_t}, \tag{4.5}$$

where $c_2 = (1-\rho_\sigma)\sigma^2$; $\boldsymbol{\omega}_{t+1} \sim N(\mathbf{0}, \boldsymbol{\Sigma}_t)$; $\boldsymbol{\Sigma}_t$ is given by Equation (2.10); and $\mathbf{c}$, $\mathbf{G}$, and $\mathbf{M}$ are functions of the DSGE model parameters in $\boldsymbol{\theta}$. We compute the model solution in Equation (4.5) via the iterative procedure described in Section 2. Using Equation (4.5), we can express the state-transition equation for the conditional Kalman filter as

$$\begin{aligned} \hat{\mathbf{x}}_t &= \mathbf{c}_1 + \mathbf{G}_{11}\hat{\mathbf{x}}_{t-1} + \mathbf{G}_{12}\sigma_{t-1}^2 + \mathbf{M}_{11}\boldsymbol{\varepsilon}_t + \mathbf{M}_{12}\underbrace{\left(\sigma_t^2 - c_2 - \rho_\sigma \sigma_{t-1}^2\right)}_{\varepsilon_{\sigma,t}} \\ &= \underbrace{\mathbf{c}_1 - c_2\mathbf{M}_{12} + \mathbf{M}_{12}\sigma_t^2 + (\mathbf{G}_{12} - \rho_\sigma \mathbf{M}_{12})\sigma_{t-1}^2}_{\tilde{\mathbf{c}}_t} + \mathbf{G}_{11}\hat{\mathbf{x}}_{t-1} + \mathbf{M}_{11}\boldsymbol{\varepsilon}_t, \end{aligned} \tag{4.6}$$

where $\boldsymbol{\varepsilon}_{t+1} \sim N(\mathbf{0}, \mathbf{H}\sigma_t^2)$. The state-transition equation in Equation (4.6) is linear and Gaussian with a time-varying intercept vector and covariance matrix.

The measurement equation for the Kalman filter corresponding to $\mathbf{s}_t$ is given by

$$\mathbf{y}_t = \mathbf{d} + \underbrace{\begin{bmatrix} \mathbf{Z}_1 & \mathbf{0} \end{bmatrix}}_{\mathbf{Z}} \underbrace{\begin{bmatrix} \hat{\mathbf{x}}_t \\ \sigma_t^2 \end{bmatrix}}_{\mathbf{s}_t} + \mathbf{u}_t, \tag{4.7}$$

where $\mathbf{u}_t \sim N(\mathbf{0}, \mathbf{\Sigma}_u)$ is a vector of measurement errors and $\mathbf{\Sigma}_u$ is the diagonal covariance matrix for $\mathbf{u}_t$. The presence of measurement errors in Equation (4.7) allows us to use more observable variables than structural shocks when estimating the DSGE model. In addition, measurement errors recognize the approximate nature of the affine solution, potential misspecification of structural equations, disparities between model and observable variables, and reporting errors by statistical agencies.[13] From Equation (4.7), the measurement equation for the conditional Kalman filter is given by

$$\mathbf{y}_t = \mathbf{d} + \mathbf{Z}_1 \hat{\mathbf{x}}_t + \mathbf{u}_t. \tag{4.8}$$

As in Section 3, we can straightforwardly use Equation (2.7) to compute the value of $p\big(\boldsymbol{\sigma}^2 \big| \boldsymbol{\theta}\big)$ in Equations (4.1) to (4.3):

$$p\big(\boldsymbol{\sigma}^2 \big| \boldsymbol{\theta}\big) = \prod_{t=1}^{T} p_{\mathcal{N}}\big(\sigma_t^2 \big| (1-\rho_\sigma)\sigma^2 + \rho_\sigma \sigma_{t-1}^2, \varphi_\sigma^2\big). \tag{4.9}$$

4.2 Second Gibbs Step

Drawing the series of common stochastic volatility components from $p\big(\boldsymbol{\sigma}^2 \big| \mathbf{Y}, \boldsymbol{\theta}\big)$ constitutes data augmentation. As in Section 3, we use Gibbs sampling and alternately draw σ_t^2 from $p\big(\sigma_t^2 \big| \boldsymbol{\sigma}_{\backslash t}^2, \mathbf{Y}, \boldsymbol{\theta}\big)$ for $t = 1, \ldots, T$. Using Bayes' theorem, we can express the posterior density for σ_t^2 as

$$p\big(\sigma_t^2 \big| \boldsymbol{\sigma}_{\backslash t}^2, \boldsymbol{\theta}, \mathbf{Y}\big) \propto p\big(\mathbf{Y} \big| \boldsymbol{\sigma}^2, \boldsymbol{\theta}\big) p\big(\sigma_{t+1}^2 \big| \boldsymbol{\sigma}_{\backslash t+1}^2, \boldsymbol{\theta}\big) p\big(\sigma_t^2 \big| \boldsymbol{\sigma}_{\backslash t,t+1}^2, \boldsymbol{\theta}\big). \tag{4.10}$$

[13] See Guerrón-Quintana (2010) on the benefits of including measurement errors in DSGE model estimation.

Ignoring components not affected by σ_t^2 and using Equation (2.7), Equation (4.10) becomes

$$p\big(\sigma_t^2\big|\boldsymbol{\sigma}_{\setminus t}^2,\boldsymbol{\theta},\mathbf{Y}\big)\propto p\Big(\{\mathbf{y}_s\}_{s=t}^T\big|\{\sigma_s^2\}_{s=t-1}^T,\boldsymbol{\theta}\Big)p_{\mathcal{N}}\big(\sigma_{t+1}^2\big|(1-\rho_\sigma)\sigma^2+\rho_\sigma\sigma_t^2,\varphi_\sigma^2\big)\cdots \\ p_{\mathcal{N}}\big(\sigma_t^2\big|(1-\rho_\sigma)\sigma^2+\rho_\sigma\sigma_{t-1}^2,\varphi_\sigma^2\big). \tag{4.11}$$

We use an analogous version of the procedure in Section 3 to draw σ_t^2 for $t=1,\ldots,T$:

(1) **Initialization** Set $\sigma_0^2=\sigma^2$; set the initial state mean vector, $\hat{\mathbf{x}}_{0|0}$, and covariance matrix, $\mathbf{P}_{0|0}$, to their steady-state values.

(2) **Recursion** For $t=1,\ldots,T-1$, compute the posterior kernel density for σ_t^2 in Equation (4.11) and sample σ_t^2 using the MH algorithm with a tailored proposal density. We use the conditional Kalman filter in Section 4.1 to compute $p\Big(\{\mathbf{y}_s\}_{s=t}^T\big|\{\sigma_s^2\}_{s=t-1}^T,\boldsymbol{\theta}\Big)$ in Equation (4.11).[14]

(3) **Terminal Condition** For $t=T$, Equation (4.11) becomes

$$p\big(\sigma_T^2\big|\boldsymbol{\sigma}_{\setminus T}^2,\boldsymbol{\theta},\mathbf{Y}\big)\propto p\Big(\mathbf{y}_T\big|\{\sigma_s^2\}_{s=T-1}^T,\boldsymbol{\theta}\Big)p_{\mathcal{N}}\big(\sigma_T^2\big|(1-\rho_\sigma)\sigma^2+\rho_\sigma\sigma_{T-1}^2,\varphi_\sigma^2\big). \tag{4.12}$$

We compute the posterior kernel density for σ_T^2 in Equation (4.12) and again sample σ_T^2 using the MH algorithm with a tailored proposal density.

We use a univariate student's t distribution with ten degrees of freedom as the proposal density for Equations (4.11) and (4.12). We make J simulated draws of the parameter vector and stochastic volatility series, denoted by $\big\{\boldsymbol{\theta}^{(j)}\big\}_{j=1}^J$ and $\big\{\boldsymbol{\sigma}^{2,(j)}\big\}_{j=1}^J$, respectively. In the next section, we employ the MCMC algorithm to estimate a DSGE model with time-preference, technology, investment, and volatility shocks.[15]

[14] Based on the most current value of σ_t^2, we compute $\hat{\mathbf{x}}_{t|t}$ and $\mathbf{P}_{t|t}$, which then serve as the initial state mean vector and covariance matrix, respectively, for the conditional Kalman filter used to compute $p\Big(\{\mathbf{y}_s\}_{s=t}^T\big|\{\sigma_s^2\}_{s=t-1}^T,\boldsymbol{\theta}\Big)$ in the next iteration of the recursion, where $\hat{\mathbf{x}}_{t|t}$ ($\mathbf{P}_{t|t}$) is the period-t state vector (covariance matrix) based on data through t.

[15] Bianchi et al. (2019) analyze term premia in a DSGE model with a two-state Markov-switching process for volatility. We view the present paper and Bianchi et al. (2019) as complements.

5 DSGE Model

5.1 Environment

The representative household (i.e., investor) has recursive preferences (Epstein and Zin 1989, 1991; Weil 1989):

$$V_t = \left\{ (1 - \upsilon_t \beta) C_t^{1-\frac{1}{\psi}} + \upsilon_t \beta \left[E_t \left(V_{t+1}^{1-\phi} \right) \right]^{\frac{1-\frac{1}{\psi}}{1-\phi}} \right\}^{\frac{1}{1-\frac{1}{\psi}}}, \tag{5.1}$$

where C_t is consumption, $0 < \beta < 1$ is the time discount factor, $\upsilon_t \in (0, 1/\beta)$ is a time-preference shock with an unconditional mean of unity, $\psi > 0$ is the EIS, and $\phi > 0$ is the RRA.[16] If $\phi = 1/\psi$, then Equation (5.1) reduces to the conventional expected power utility specification, and the investor is indifferent to the timing of risk resolution. When $\phi \neq 1/\psi$, recursive preferences generate a preference for the timing of risk resolution: the investor prefers the early (late) resolution of risk when $\phi > (<) \, 1/\psi$.

The time-preference shock υ_t in Equation (5.1) can be viewed as a "demand" shock. Smets and Wouters (2003), Christiano et al. (2011), and Basu and Bundick (2017) include time-preference shocks in DSGE models; Gourio (2012) shows that a shock to the probability of a disaster can be interpreted as a time-preference shock. The particular way in which υ_t enters Equation (5.1) follows the specification of de Groot et al. (2018) to ensure that the distributional weights on current and future utility sum to unity.[17] The log of υ_t follows a stationary AR process:

$$\log(\upsilon_{t+1}) = \rho_\upsilon \log(\upsilon_t) + \underbrace{\varphi_\upsilon \sigma_t e_{\upsilon,t+1}}_{\varepsilon_{\upsilon,t+1}}, \tag{5.2}$$

where $0 \leq \rho_\upsilon < 1$, $\varphi_\upsilon \geq 0$, σ_t^2 is the common stochastic volatility component for the shocks in the model, $e_{\upsilon,t} \sim$ i.i.d. $\mathcal{N}(0,1)$, and σ_t^2 obeys the AR process in Equation (2.7).

[16] As in Kaltenbrunner and Lochstoer (2010), we impose the restriction that $\psi \neq 1$ but allow for ψ values arbitrarily close to unity.

[17] If the sum of the distributional weights is not restricted to unity, de Groot et al. (2018) show that troublesome asymptotes exist in the impulse responses to a time-preference shock.

The household supplies labor services, N_t, to the representative firm and receives a real wage, W_t, per unit of labor services. The household is also a shareholder in the representative firm, so that it receives a real dividend, D_t, from the firm. With these sources of funds, the household's budget constraint is given by

$$C_t + a_{t+1}P_t = W_t N_t + a_t(P_t + D_t), \tag{5.3}$$

where a_t is the number of equity shares held by the household (at the beginning of period t) and P_t is the real price of an equity share.[18]

The representative firm operates in a competitive environment and chooses capital and labor to maximize the expected value of the firm to its shareholder (i.e., the household). The expected value of the firm is equal to the present discounted value of current and expected future cash flows:

$$\Xi_t = E_t\left\{\sum_{s=0}^{\infty} M_{t+s,t}[F(K_{t+s}, A_{t+s}L_{t+s}) - W_{t+s}L_{t+s} - I_{t+s}]\right\}, \tag{5.4}$$

where $M_{t+s,t} = \prod_{k=1}^{s} M_{t+k,t+k-1}$ for $s > 1$, $M_{t+1,t}$ is the household's intertemporal marginal rate of substitution between periods t and $t+1$ (i.e., the SDF), $M_{t,t} = 1$, L_t is labor employed by the firm, K_t is the capital stock, and I_t is investment. The firm takes the household's SDF as exogenous.

The firm produces output via a Cobb-Douglas production function:

$$Y_t = F(K_t, A_t L_t) = K_t^{\alpha}(A_t L_t)^{1-\alpha}, \tag{5.5}$$

where $0 < \alpha < 1$ and A_t is labor-augmenting technology. Labor-augmenting technology evolves according to

$$A_{t+1} = z_{t+1}\gamma A_t, \tag{5.6}$$

[18] We assume that markets are complete.

where $\gamma \geq 1$ is the deterministic gross growth rate of A_t and z_t is a technology shock with an unconditional mean of unity. The log of z_t follows a stationary AR process:

$$\log(z_{t+1}) = \rho_z \log(z_t) + \underbrace{\sigma_t e_{z,t+1}}_{\varepsilon_{z,t+1}}, \tag{5.7}$$

where $0 \leq \rho_z < 1$ and $e_{z,t} \sim$ i.i.d. $\mathcal{N}(0,1)$.

Capital accumulation by the firm is subject to capital adjustment costs:

$$K_{t+1} = (1-\delta)K_t + \nu_t \kappa(I_t/K_t)K_t, \tag{5.8}$$

where

$$\kappa(I_t/K_t) = a_1 + \left(\frac{a_2}{1-\frac{1}{\chi}}\right)\left(\frac{I_t}{K_t}\right)^{1-\frac{1}{\chi}} \tag{5.9}$$

is the specification from Jermann (1998), $0 < \delta < 1$ is the rate of depreciation, $\chi > 0$ is the elasticity of investment with respect to Tobin's q, and ν_t is an investment shock with an unconditional mean of unity.[19] A lower (higher) value of χ corresponds to higher (lower) capital adjustment costs. Following Jermann (1998), we set a_1 and a_2 so that there are no adjustment costs in the steady state. The log of ν_t evolves as a stationary AR process:

$$\log(\nu_{t+1}) = \rho_\nu \log(\nu_t) + \underbrace{\varphi_\nu \sigma_t e_{\nu,t+1}}_{\varepsilon_{\nu,t+1}}, \tag{5.10}$$

where $0 \leq \rho_\nu < 1$, $\varphi_\nu \geq 0$, and $e_{\nu,t} \sim$ i.i.d. $N(0,1)$.[20]

The firm does not issue new shares, so that it solely accumulates capital via retained earnings. We normalize the number of shares outstanding to unity ($a_t = 1$ for all t). After

[19] Greenwood et al. (1988), Justiniano et al. (2010, 2011), and Liu et al. (2011) find that shocks to capital accumulation contribute significantly to US business-cycle fluctuations.

[20] In the endowment economies of Bansal and Yaron (2004) and related studies, the reduced-form consumption and dividend growth processes share a common stochastic volatility component. In our model, the structural shocks in Equations (5.2), (5.7) and (5.10) share the common stochastic volatility component in Equation (2.7), so that our modeling of time-varying macroeconomic volatility is a natural extension of Bansal and Yaron (2004) to a DSGE production economy.

paying for labor services and financing its investment spending out of retained earnings, the firm pays a dividend of

$$D_t = Y_t - W_t L_t - I_t \tag{5.11}$$

to the household.

5.2 Equilibrium Conditions

For the utility specification given by Equation (5.1), the Internet Appendix shows that the household's SDF can be expressed as

$$M_{t+1,t} = \left[\upsilon_t \beta \left(\frac{1-\upsilon_{t+1}\beta}{1-\upsilon_t \beta}\right)\right]^{\zeta} \left(\frac{C_{t+1}}{C_t}\right)^{-\frac{1}{\psi}\zeta} R_{w,t+1}^{\zeta-1}, \tag{5.12}$$

where

$$\zeta = \frac{1-\phi}{1-\frac{1}{\psi}}, \tag{5.13}$$

$$R_{w,t+1} = \frac{J_{t+1}}{J_t - C_t}, \tag{5.14}$$

and J_t is the real value of aggregate wealth (including C_t). Equation (5.14) is the gross return on aggregate wealth, which represents a claim to the household's consumption stream.

Because leisure does not enter the utility function, the household allocates its entire time endowment, which we normalize to unity, to market work, so that $N_t = L_t = 1$ for all t. As financial market equilibrium requires that the household holds all outstanding shares (and recalling that $a_t = 1$ for all t), the budget constraint in Equation (5.3) becomes

$$C_t = W_t + D_t. \tag{5.15}$$

All other assets are held in zero net supply in equilibrium.[21] We also have the resource constraint that all output is either consumed or invested:

$$Y_t = C_t + I_t. \tag{5.16}$$

Optimal shareholding by the household gives rise to the familiar Euler equation:

$$E_t(M_{t+1,t}R_{t+1}) = 1, \tag{5.17}$$

where

$$R_{t+1} = \frac{P_{t+1} + D_{t+1}}{P_t} \tag{5.18}$$

is the gross return on equity. An analogous relationship holds for aggregate wealth:

$$E_t(M_{t+1,t}R_{w,t+1}) = 1. \tag{5.19}$$

We also define the gross return on human wealth:

$$R_{h,t+1} = \frac{H_{t+1} + W_{t+1}}{H_t}, \tag{5.20}$$

where H_t is the real value of human wealth, and based on the definition of J_t:

$$H_t = J_t - P_t - D_t - W_t. \tag{5.21}$$

Turning to the firm, maximizing Equation (5.4) subject to Equations (5.5) and (5.8) yields the firm's optimal labor choice,

$$(1 - \alpha)Y_t = W_t, \tag{5.22}$$

[21] Strictly speaking, the household also holds all outstanding shares of human wealth, where we again normalize the number of shares outstanding to unity. In equilibrium, Equation (5.15) continues to hold.

as well as its Euler equation,

$$E_t(M_{t+1,t}R_{i,t+1}) = 1, \tag{5.23}$$

where

$$R_{i,t+1} = \frac{\alpha Y_{t+1}}{q_t K_{t+1}} + \frac{q_{t+1}}{q_t}\left\{(1-\delta) + \nu_{t+1}\left[a_1 + \left(\frac{a_2}{\chi - 1}\right)\left(\frac{I_{t+1}}{K_{t+1}}\right)^{1-\frac{1}{\chi}}\right]\right\} \tag{5.24}$$

is the firm's gross return on investment and

$$q_t = \left(\frac{1}{\nu_t a_2}\right)\left(\frac{I_t}{K_t}\right)^{\frac{1}{\chi}} \tag{5.25}$$

is Tobin's marginal q. The model satisfies the conditions in Proposition 1 of Hayashi (1982), so that marginal q is equal to average q. As shown by Restoy and Rockinger (1994), the Hayashi (1982) conditions imply that the return on a share of equity coincides with the firm's return on investment ($R_{t+1} = R_{i,t+1}$), so that the household's and firm's Euler equations—Equations (5.17) and (5.23)—coincide; Restoy and Rockinger (1994) also show that the Hayashi (1982) conditions imply that

$$P_t = K_{t+1}q_t. \tag{5.26}$$

Equation (5.6) induces stochastic trend growth in Y_t, C_t, I_t, K_t, W_t, J_t, P_t, D_t, and H_t, so that we detrend these variables relative to A_t. It is also convenient to work with detrended versions of Equations (5.14), (5.18) and (5.20). The remaining variables in the model (q_t, υ_t, ν_t, z_t, σ_t^2) are stationary. The Internet Appendix provides the 17 equations comprising the model in terms of the twelve detrended and five remaining variables.

5.3 Affine Solution

As shown in the Internet Appendix, a log-linearized approximation of the SDF is given by

$$\begin{aligned} m_{t+1,t} = \log(\beta) - \frac{1}{\psi}\log(\gamma) - \zeta\left(\frac{\beta}{1-\beta}\right)\hat{v}_{t+1} + \zeta\left(\frac{1}{1-\beta}\right)\hat{v}_t \\ - \frac{1}{\psi}\zeta(\hat{c}_{t+1} - \hat{c}_t) + (\zeta - 1)\hat{r}_{w,t+1} - \phi\hat{z}_{t+1}, \end{aligned} \tag{5.27}$$

where a "ˆ" denotes log deviation from the non-stochastic steady state and $m_{t+1,t} = \log(M_{t+1,t})$. Using Equation (5.27), the Euler equation for aggregate wealth can be expressed in logs as

$$\begin{aligned} \log\Bigg(E_t\Bigg\{\exp\Bigg[\zeta\hat{r}_{w,t+1} - \frac{1}{\psi}\zeta(\hat{c}_{t+1} - \hat{c}_t) - \zeta\left(\frac{\beta}{1-\beta}\right)\hat{v}_{t+1} \\ + \zeta\left(\frac{1}{1-\beta}\right)\hat{v}_t + \left(1 - \frac{1}{\psi}\right)\zeta\hat{z}_{t+1}\Bigg]\Bigg\}\Bigg) = 0, \end{aligned} \tag{5.28}$$

while that for equity is given by

$$\begin{aligned} \log\Bigg(E_t\Bigg\{\exp\Bigg[(\zeta - 1)\hat{r}_{w,t+1} - \frac{1}{\psi}\zeta(\hat{c}_{t+1} - \hat{c}_t) + \hat{r}_{t+1} - \zeta\left(\frac{\beta}{1-\beta}\right)\hat{v}_{t+1} \\ + \zeta\left(\frac{1}{1-\beta}\right)\hat{v}_t + \left(1 - \frac{1}{\psi}\right)\zeta\hat{z}_{t+1}\Bigg]\Bigg\}\Bigg) = 0. \end{aligned} \tag{5.29}$$

Conjecturing the affine solution in Equation (2.5) and exploiting log-normality, we can write the Euler equations for aggregate wealth and equity as

$$\begin{aligned} E_t(\hat{r}_{w,t+1}) - \frac{1}{\psi}[E_t(\hat{c}_{t+1}) - \hat{c}_t] + \left(\frac{1 - \beta\rho_v}{1-\beta}\right)\hat{v}_t + \left(1 - \frac{1}{\psi}\right)\rho_z\hat{z}_t \\ + 0.5\,\zeta\left[\boldsymbol{\eta}'_{r_w} - \frac{1}{\psi}\boldsymbol{\eta}'_c - \left(\frac{\beta}{1-\beta}\right)\boldsymbol{\eta}'_v + \left(1 - \frac{1}{\psi}\right)\boldsymbol{\eta}'_z\right]\mathbf{M}\boldsymbol{\Sigma}_t\mathbf{M}'\cdots \\ \left[\boldsymbol{\eta}'_{r_w} - \frac{1}{\psi}\boldsymbol{\eta}'_c - \left(\frac{\beta}{1-\beta}\right)\boldsymbol{\eta}'_v + \left(1 - \frac{1}{\psi}\right)\boldsymbol{\eta}'_z\right]' = 0 \end{aligned} \tag{5.30}$$

and

$$
\begin{aligned}
&(\zeta-1)E_t(\hat{r}_{w,t+1})-\frac{1}{\psi}\zeta[E_t(\hat{c}_{t+1})-\hat{c}_t]+E_t(\hat{r}_{t+1})+\zeta\left(\frac{1-\beta\rho_v}{1-\beta}\right)\hat{v}_t+(1-\phi)\rho_z\hat{z}_t \\
&+0.5\left[(\zeta-1)\boldsymbol{\eta}'_{r_w}-\frac{1}{\psi}\zeta\boldsymbol{\eta}'_c+\boldsymbol{\eta}'_r-\zeta\left(\frac{\beta}{1-\beta}\right)\boldsymbol{\eta}'_v+(1-\phi)\boldsymbol{\eta}'_z\right]\mathbf{M}\boldsymbol{\Sigma}_t\mathbf{M}'\cdots \\
&\quad\left[(\zeta-1)\boldsymbol{\eta}'_{r_w}-\frac{1}{\psi}\zeta\boldsymbol{\eta}'_c+\boldsymbol{\eta}'_r-\zeta\left(\frac{\beta}{1-\beta}\right)\boldsymbol{\eta}'_v+(1-\phi)\boldsymbol{\eta}'_z\right]'=0,
\end{aligned}
\tag{5.31}
$$

respectively, where $\boldsymbol{\eta}_{\cdot}$ is an N-dimensional vector with a one in the row corresponding to the variable from $\mathbf{s}_t$ in the subscript and zeros elsewhere, and

$$
\boldsymbol{\Sigma}_t=\begin{bmatrix}\varphi_v^2\sigma_t^2 & 0 & 0 & 0\\ 0 & \varphi_\nu^2\sigma_t^2 & 0 & 0\\ 0 & 0 & \sigma_t^2 & 0\\ 0 & 0 & 0 & \varphi_\sigma^2\end{bmatrix}. \tag{5.32}
$$

Observe that Equations (5.30) and (5.31) are affine functions of $E_t(\hat{r}_{w,t+1})$, $E_t(\hat{c}_{t+1})$, $E_t(\hat{r}_{t+1})$, $\hat{c}_t$, $\hat{v}_t$, $\hat{z}_t$, and σ_t^2.

The Internet Appendix gives the log-linearized approximations of the eleven non-Euler equations. The Euler equations in Equations (5.30) and (5.31); log-linearized approximations to the non-Euler equations; and Equations (2.7), (5.2), (5.7) and (5.10) constitute an affine system of expectational difference equations in the model variables. As described in Section 2, we solve the system via an iterative procedure based on Gensys.[22]

Under log-normality, the general expression for the log equity risk premium is given by

$$
E_t(r_{t+1})-r_{f,t+1}=-0.5\mathrm{Var}_t(r_{t+1})-\mathrm{Cov}_t(m_{t+1,t},r_{t+1}), \tag{5.33}
$$

[22]Pohl et al. (2018) analyze affine solution approximations for the Bansal and Yaron (2004) endowment economy specification and variants thereof. When the reduced-form shock and stochastic volatility processes are highly persistent, Pohl et al. (2018) find that affine approximations can omit significant nonlinearities in the complete model solution (approximated via projection methods). Although our DSGE framework is not directly comparable to the endowment economy specifications analyzed in Pohl et al. (2018), they find only small approximation errors for the affine solution when the AR parameter for the stochastic volatility process is not close to unity, which is the case for the estimated DSGE model in Section 6.

where $r_t = \log(R_t)$. Based on Equations (2.5) and (5.27), Equation (5.33) can be expressed as

$$\begin{aligned} E_t(r_{t+1}) - r_{f,t+1} = & -0.5(\boldsymbol{\eta}_r' + \boldsymbol{\eta}_z')\mathbf{M}\boldsymbol{\Sigma}_t\mathbf{M}'(\boldsymbol{\eta}_r' + \boldsymbol{\eta}_z')' \\ & - \left[(\zeta - 1)\boldsymbol{\eta}_{r_w}' - \frac{1}{\psi}\zeta\boldsymbol{\eta}_c' - \zeta\left(\frac{\beta}{1-\beta}\right)\boldsymbol{\eta}_v' - \phi\boldsymbol{\eta}_z'\right]\cdots \\ & \mathbf{M}\boldsymbol{\Sigma}_t\mathbf{M}'(\boldsymbol{\eta}_r' + \boldsymbol{\eta}_z')'. \end{aligned} \tag{5.34}$$

The risk-adjusted steady-state log equity risk premium is given by Equation (5.34) evaluated at $\boldsymbol{\Sigma}_t = \boldsymbol{\Sigma}$, where

$$\boldsymbol{\Sigma} = \begin{bmatrix} \varphi_\upsilon^2\sigma^2 & 0 & 0 & 0 \\ 0 & \varphi_\nu^2\sigma^2 & 0 & 0 \\ 0 & 0 & \sigma^2 & 0 \\ 0 & 0 & 0 & \varphi_\sigma^2 \end{bmatrix}. \tag{5.35}$$

Stochastic volatility produces a time-varying equity risk premium in Equation (5.34) via time variation in the quantity of macroeconomic risk, as captured by σ_t^2.

6 Estimation Results

6.1 Data

We estimate the DSGE model using five observable variables: log equity market excess return (EXR_t), ex ante log real risk-free return (RFR_t), real per capita consumption log growth (CGR_t), real per capita investment log growth (IGR_t), and real per capita compensation log growth (WGR_t). The data are quarterly for 1973:1 to 2018:4. The 1973:1 starting point accommodates the apparent change in US productivity growth beginning around that time (e.g., Gordon 2016).

Table 1 reports summary statistics for the observable variables. The large average equity market excess return (1.23%, 4.92% annualized) and its substantial volatility (8.25%, 16.50%

annualized), along with the much smaller average risk-free return (0.34%) and its limited volatility (0.57%), underlie the equity risk premium and risk-free rate puzzles (Mehra and Prescott 1985; Weil 1989), respectively. The risk-free return is considerably more persistent than the equity market excess return (autocorrelation coefficients of 0.94 and 0.09, respectively). Average consumption, investment, and compensation growth range from 0.38% to 0.52%. Among the non-return variables, investment growth exhibits the highest volatility (2.87%), followed by compensation (0.80%) and consumption (0.49%) growth. Consumption, investment, and compensation growth are moderately persistent (autocorrelation coefficients of 0.44, 0.41, and 0.35, respectively). The summary statistics in Table 1 reflect well-known characteristics of asset return and macroeconomic data.

The measurement equation is given by

$$\underbrace{\begin{bmatrix} \text{EXR}_t \\ \text{RFR}_t \\ \text{CGR}_t \\ \text{IGR}_t \\ \text{WGR}_t \end{bmatrix}}_{\mathbf{y}_t} = \begin{bmatrix} 0 \\ \frac{1}{\psi}\log(\gamma) - \log(\beta) \\ \log(\gamma) \\ \log(\gamma) \\ \log(\gamma) \end{bmatrix} + \begin{bmatrix} \vartheta(\hat{r}_t + \hat{z}_t - \hat{r}_{f,t}) \\ \hat{r}_{f,t} \\ \hat{c}_t - \hat{c}_{t-1} + \hat{z}_t \\ \hat{i}_t - \hat{i}_{t-1} + \hat{z}_t \\ \hat{w}_t - \hat{w}_{t-1} + \hat{z}_t \end{bmatrix} + \mathbf{u}_t. \tag{6.1}$$

Following Croce (2014) and Hirshleifer et al. (2015), the parameter $\vartheta > 0$ in the first equation of Equation (6.1) accommodates the fact that excess returns are levered in the data. We set the square root of each element of the main diagonal of $\mathbf{\Sigma}_u$ to 20% of the sample standard deviation of the respective element in $\mathbf{y}_t$.

6.2 Priors

Following standard practice, we fix the values for α and δ at 0.36 and 0.025, respectively. The second through fourth columns of Table 2 report the marginal prior distributions for

the remaining parameters. We effectively truncate the joint prior distribution by restricting the parameters to the region where a unique solution to the DSGE model exists.

We use Gamma prior distributions for ψ, ϕ, and χ, which impose the non-negativity constraints for the parameters. The prior mean for ψ is two, which is used in a number of recent calibrations (e.g., Ai 2010; Gourio 2012; Bansal et al. 2014; Croce 2014; Hirshleifer et al. 2015; Favilukis and Lin 2016). Together with the prior mean, the prior standard deviation of 0.30 for ψ reflects a strong prior view that the EIS is above unity, consistent with the literature initiated by Bansal and Yaron (2004). The prior distribution for ϕ (mean of six, standard deviation of two) reflects a prior view that the RRA is "moderate." This prior aligns with the RRA values of six, five, five, 7.5, and 6.5 used by Guvenen (2009), Kaltenbrunner and Lochstoer (2010), Bansal et al. (2014), Chen (2016), and Favilukis and Lin (2016), respectively, in recent calibrations. The prior distribution for χ (mean of 1.5, standard deviation of 0.5) is in line with the value of 1.5 used by Hirshleifer et al. (2015) and range of values in Favilukis and Lin (2016) in their calibrations. The relatively informed priors for ψ, ϕ, and χ serve as regularization devices for helping to keep the posterior estimates in what can be viewed as economically plausible regions of the parameter space.

To facilitate scaling, we express the priors for β and γ in terms of $r^{\mathrm{Q}} = 100[(1/\beta) - 1]$ and $\gamma^{\mathrm{Q}} = 100(\gamma - 1)$, respectively. We again use Gamma prior distributions for r^{Q} and γ^{Q} to impose the relevant sign restrictions. For r^{Q}, we specify a prior mean of 0.3, which corresponds to a β value of 0.997 and an annualized growth- and risk-unadjusted steady-state risk-free return of 1.2%. The prior mean for γ^{Q} is 0.4, which translates to a γ value of 1.004. We set the prior standard deviations for both r^{Q} and γ^{Q} to 0.1.

To impose the stationarity restrictions, we use Beta prior distributions for the AR parameters in Equations (2.7), (5.2), (5.7) and (5.10). Similarly to Del Negro et al. (2007), the priors for ρ_υ, ρ_ν, and ρ_σ are fairly tightly concentrated around 0.8. As the technology shock corresponds to the growth rate of labor-augmenting technology, we center the distribution for ρ_z at 0.2. Gamma distributions, which impose the relevant sign restrictions, serve as the

priors for the volatility scaling parameters, φ_υ and φ_ν. We set the prior means to one and standard deviations to 0.5 for these distributions, reflecting relatively uninformed priors.

Inverse-Gamma Type 1 distributions serve as the prior distributions for σ and φ_σ. To facilitate scaling, we express the priors in terms of $\sigma \times 10^2$ and $\varphi_\sigma \times 10^4$, respectively. The prior for $\sigma \times 10^2$ is approximately centered on 0.5. In conjunction with the prior mean of 0.2 for ρ_z, this value corresponds to an unconditional standard deviation of about 0.5% for the growth rate of labor-augmenting technology. We center the prior mean for $\varphi_\sigma \times 10^4$ near 0.06, which helps to prevent σ_t^2 from becoming negative.

Finally, we use a Gamma prior distribution for the leverage factor ϑ. The prior mean of 1.5 is close to the value of 1.67 used by Hirshleifer et al. (2015) in their calibrations, which they indicate is based on the debt-equity ratio reported in Benninga and Protopapadakis (1990). The prior standard deviation of 0.1 for ϑ represents a relatively tight prior that is designed to help prevent an inordinately large leverage factor from trivially "explaining" the US equity risk premium.

6.3 Posterior Estimates

The fifth and sixth columns of Table 2 report means and 90% credible probability intervals, respectively, for the posterior distributions for the DSGE model parameters.[23] The results are based on 10,000 draws (after 5,000 burn-in draws) generated by the MCMC algorithm in Section 4. The number of draws is substantially smaller than that typically used for the conventional random-walk MH algorithm, reflecting the increased efficiency achieved by tailoring the proposal densities. Evidence of the efficiency of the algorithm is provided in the last column of Table 2, which reports the inefficiency factors for the sequence of posterior draws for each parameter. The inefficiency factors are all relatively small (ranging from 20.8 to 62.6), indicating that the Markov chain mixes well.

[23] All of the credible probability intervals are highest posterior density intervals.

The posterior mean for ψ is 1.79 in Table 2. The posterior 90% credible probability interval supports an EIS value significantly above unity, and it includes the popular value of two used in recent calibrations with recursive preferences. The posterior mean for ϕ, 10.30, is larger than the values used in Guvenen (2009), Kaltenbrunner and Lochstoer (2010), Bansal et al. (2014), Chen (2016), and Favilukis and Lin (2016); nevertheless, the posterior estimate represents a reasonably moderate RRA and is very close to the Bansal and Yaron (2004) benchmark value of ten, which is also used by Croce (2014).[24] In sum, although the results for ϕ in Table 2 indicate a more sizable RRA than assumed in some recent calibrations, the RRA still appears fairly moderate. Combined with the posterior estimate for ψ, the posterior estimate for ϕ implies that the representative investor has a preference for the early resolution of risk ($\phi > 1/\psi$).

The posterior mean for χ is 0.31, indicating substantial capital adjustment costs. The 90% credible interval for χ is well below the prior mean of 1.5, so that the data strongly favor significant adjustment costs in the context of the DSGE model. As pointed out by Jermann (1998), capital adjustment costs help to produce a sizable equity risk premium in a production economy: with small (or no) capital adjustment costs, it is relatively easy for agents to adjust their production plans to smooth consumption; substantive capital adjustment costs make it more difficult for agents to smooth consumption, thereby exposing them to greater macroeconomic risk and generating a higher equity risk premium.

The posterior estimates appear plausible for the remaining parameters in Table 2. The posterior means for ρ_υ and ρ_ν are both above 0.95, so that the time-preference and investment shocks are quite persistent. Consistent with a shock to the growth rate of labor-augmenting technology, the technology shock is much less persistent (posterior mean of 0.12 for ρ_z). The posterior mean for ρ_σ is 0.84. Although this value signals considerable persistence in the common stochastic volatility component, it is smaller than the values typically found in studies of recursive preferences in the context of endowment economies; for example, Bansal

[24]The 90% credible interval also includes the value of nine used by Nakamura et al. (2017).

and Yaron (2004) specify a monthly autoregressive parameter of 0.987 for their stochastic volatility process, which translates into a quarterly value of $0.987^3 = 0.96$ and falls outside of the 90% credible interval for ρ_σ in Table 2. The posterior mean of 1.78 for ϑ indicates that an outsized leverage factor is not responsible for the equity risk premium in the estimated DSGE model.[25]

Figure 1 provides additional information on the common stochastic volatility component in the DSGE model. The figure shows the estimated historical stochastic volatility series for 1973:1 to 2018:4 based on the $\boldsymbol{\sigma}^2$ draws generated by the data augmentation step of the Gibbs sampler. The solid line is the posterior mean of σ_t (in percent), while the bands delineate posterior 90% credible intervals. The stochastic volatility series displays pronounced countercyclical fluctuations in Figure 1, with marked increases in volatility accompanying the recessions in the mid 1970s, early 1990s, and early 2000s, as well as the recent Great Recession. Volatility is low by historical standards throughout much of the 1980s, mid-to-late 1990s, and mid 2000s, so that the Great Moderation (Stock and Watson 2002) is evident to a degree in Figure 1.

7 Determinants of the Equity Risk Premia

This section investigates the determinants of the equity risk premium in the estimated DSGE model.[26] Recalling Equation (5.33), a positive and sizable log equity risk premium requires a negative and large (in magnitude) covariance between log SDF and log equity return innovations. Intuitively, the representative investor requires a positive risk premium for an asset that performs poorly during "bad times" (i.e., when marginal utility and thus the SDF

[25]The Internet Appendix reports posterior predictive distributions based on the estimated DSGE model for the summary statistics in Table 1. The posterior predictive means and p-values indicate that the DSGE model accounts the for sample means, volatilities, and autocorrelations of the equity market excess return and risk-free return. Although controversial from a "pure" Bayesian point of view (e.g., Geweke 2010), Faust and Gupta (2012) argue that posterior predictive analysis is a valuable tool for the evaluation and development of DSGE models.

[26]The Internet Appendix discusses the determinants of the ex ante risk-free return in the estimated DSGE model.

are high). Approximating the log of the SDF in Equation (5.12) by

$$\begin{aligned} m_{t+1,t} = &\zeta \log(\beta) - \zeta\left(\frac{\beta}{1-\beta}\right)\log(\upsilon_{t+1}) + \zeta\left(\frac{1}{1-\beta}\right)\log(\upsilon_t) \\ &- \frac{1}{\psi}\zeta[\log(C_{t+1}) - \log(C_t)] + (\zeta - 1)\log(R_{w,t+1}), \end{aligned} \tag{7.1}$$

it is evident that innovations to the log SDF depend on the contemporaneous responses of consumption log growth and the aggregate wealth log return to the underlying structural shocks. Evaluated at the posterior means for ψ and ϕ in Table 2, the coefficients on $\log(C_{t+1}/C_t)$ and $\log(R_{w,t+1})$ in Equation (7.1) equal 11.77 and -22.07, respectively.[27] In addition to their indirect effects via the responses of $\log(C_{t+1}/C_t)$ and $\log(R_{w,t+1})$, time-preference shocks directly affect log SDF innovations via $\log(\upsilon_{t+1})$ in Equation (7.1).

To glean insight into the underlying causes of the equity risk premium in the estimated DSGE model, Figure 2 depicts the responses of consumption growth, the return on aggregate wealth, SDF, and return on equity (all in logs multiplied by 100) to each of the four structural shocks.[28] The responses in the periods after the shock represent changes in expected values conditional on the shock.

The first column of Figure 2 displays the responses to a time-preference shock. The shock represents an increase in the value attached to the future relative to the present by the representative investor. In line with this shift in time preference, Panel A shows that consumption growth falls at the time of the shock, followed by a persistent increase. Panel E indicates a sharp contemporaneous increase in the return on aggregate wealth, consistent with the persistent increase in expected consumption growth in Panel A. Because $\zeta < 0$, the coefficient on $\log(\upsilon_{t+1})$ is positive in Equation (7.1), so that the time-preference shock directly increases the SDF; however, the contemporaneous decrease (increase) in consumption growth (the return on aggregate wealth) drives down the SDF, so that on net the SDF falls sharply

[27]Note that $-(1/\psi)\zeta + (\zeta - 1) = -\phi$, so that the sum of the coefficients on $\log(C_{t+1}/C_t)$ and $\log(R_{w,t+1})$ equals the negative of the RRA. This sum corresponds to the contemporaneous change in the SDF given a unit increase in contemporaneous consumption growth with no change in expected consumption growth.

[28]Figure 2 also shows human wealth return responses. We discuss these responses in the Internet Appendix in the context of the determinants of the human wealth risk premium.

at the time of the shock, as shown in Panel I. The representative investor's effort to save more increases the demand for equity, leading to a contemporaneous increase in the return on equity in Panel M. Taking the contemporaneous responses in Panels I and M together, time-preference shocks are a potent source of a large equity risk premium, as they generate strong negative covariation between SDF and equity return innovations.

Figure 3 furnishes additional insight into the economic mechanisms at work. The figure shows the responses of output, consumption, investment, dividends, and compensation to each of the structural shocks. The first column displays the responses to a time-preference shock. Because the capital stock is initially unchanged, output is also unchanged at the time of the shock in Panel A. The economy reallocates output from consumption (Panel E) to investment (Panel I), with the representative firm financing the increase in investment by reducing dividends (Panel M). The increase in investment leads to an increase in the capital stock and thus output over time in Panel A. The increase in the capital stock raises the marginal product of labor, so that compensation increases in Panel Q. Because the time-preference shock is highly persistent, the responses to the shock remain significant for an extended period in Figure 3, although they eventually abate.

According to the second column of Figure 2, an investment shock contributes to a negative equity risk premium. The shock induces a contemporaneous decline in consumption growth and subsequent increase in expected consumption growth (Panel B), along with a contemporaneous decline in the SDF (Panel J). The investment shock makes capital more abundant going forward, so that the return on equity falls (Panel N) at the time of the shock. By simultaneously depressing the SDF and return on equity, an investment shock creates positive covariation between SDF and equity return innovations; in the context of an investment shock, equity thus acts as a hedge against bad times and earns a negative risk premium. The responses to an investment shock in the second column of Figure 3 are qualitatively similar to those corresponding to a time-preference shock in the first column: both shocks spur investment and capital accumulation. The difference is that a time-preference

shock increases the demand for capital and thus increases the contemporaneous price of equity, while an investment shock increases the supply of capital and thus decreases the price of equity.

The third column of Figure 2 shows the responses to a technology shock. Contemporaneous and expected consumption growth increase in Panel C. The return on aggregate wealth increases at the time of the shock (Panel G), which helps to produce a contemporaneous drop in the SDF (Panel K). The return on equity increases (Panel O), reflecting the increase in the marginal product of capital. By generating contemporaneous SDF and equity return responses of opposite signs, technology shocks produce negative covariation between SDF and equity return innovations, contributing to a positive equity risk premium. A technology shock engenders contemporaneous increases in consumption and investment in Panels G and K, respectively, of Figure 3. Consumption then continues to increase over time to a permanently higher level, in line with the permanent increase in output (Panel C), so that expected consumption growth increases in response to the shock (as shown in Panel C of Figure 2). Because technology shocks are the source of the stochastic trend in the model, all of the variables in the third column of Figure 3 settle at permanently higher levels.

The responses to a volatility shock are shown in the last column of Figure 2. The shock elicits a contemporaneous decrease in consumption growth in Panel D, although the response is relatively small. Expected consumption growth increases, but the response is again relatively limited. The return on aggregate wealth falls at the time of the shock (Panel H), helping to increase the SDF at the time of the shock (Panel L). Similarly to a time-preference shock, the volatility shock raises the demand for capital due to the representative investor's desire to save more, causing a contemporaneous increase in the return on equity in Panel P. As the contemporaneous SDF and equity return responses to a volatility shock are both positive, volatility shocks contribute to a negative equity risk premium. The responses to a volatility shock in the final column of Figure 3 are qualitatively similar to those to time-

preference and investment shocks in the first and second columns, respectively, although they are less persistent and considerably smaller in magnitude.

The posterior mean for the steady-state log equity risk premium is 1.37%, with a posterior 90% credible probability interval of $[1.00\%, 1.73\%]$. The posterior means and 90% credible probability intervals for the components (in percent) attributable to each structural shock are as follows:

- Time-preference shock: 1.15 $[0.87, 1.40]$
- Investment shock: -0.53 $[-0.76, -0.29]$
- Technology shock: 0.78 $[0.45, 1.09]$
- Volatility shock: -0.03 $[-0.05, -0.01]$

Consistent with the SDF and equity return responses in Figure 2, time-preference shocks are the most important component of the steady-state equity risk premium, followed by technology shocks, while the components attributable to investment and volatility shocks are negative (although the magnitude is considerably smaller for the latter).

The effects of volatility shocks on the equity risk premium are not limited to the steady-state decomposition, as volatility shocks also generate time variation in the equity risk premium; see Equation (5.34). Figure 4 portrays the estimated historical log equity risk premium (in annualized percent) for the DSGE model. Because of the temporal link between stochastic volatility and the equity risk premium, the fluctuations in the equity risk premium in Figure 4 follow the same pattern as those in the common stochastic volatility component in Figure 1. In particular, the estimated equity risk premium series displays the same pronounced countercyclical behavior as the estimated volatility series. Figure 4 indicates that the annualized equity risk premium typically increases by approximately 600 basis points during recessions. For example, according to the posterior mean, the annualized equity risk

premium goes from near 1% in early 2007 before the start of the Great Recession to around 7% in 2009 in the wake of the Great Recession.[29]

Overall, Figure 4 paints a plausible picture of the time-varying equity risk premium. The countercyclical fluctuations in the equity risk premium mesh with results from studies of stock return predictability based on predictive regressions (e.g., Fama and French 1989; Cooper and Priestly 2009; Rapach et al. 2010), and the magnitudes of the swings in the required excess return over the business cycle are economically significant. In the context of the estimated DSGE model, the equity risk premium rises during economic contractions, due to an increase in macroeconomic risk stemming from greater volatility in the underlying structural shocks buffeting the economy.

8 Conclusion

We develop an MCMC algorithm the employs an affine solution based on log-normality and tailored proposal densities to make the estimation of risk premia in DSGE models with stochastic volatility computationally feasible and efficient. To assist researchers, a `MATLAB` toolbox that implements the MCMC algorithm is publicly available. We apply our MCMC algorithm to analyze the determinants of the US equity risk premium in a DSGE model with time-preference, technology, investment, and volatility shocks, and we find that time-preference and technology shocks are the key drivers of the large equity risk premium in the estimated model. The estimated historical stochastic volatility series evinces marked countercyclical fluctuations, which give rise to countercyclical fluctuations in the equity risk premium.

[29] In a DSGE model with constant volatility, Rudebusch and Swanson (2012) show that higher-order solutions generate time variation in the term premium. With expected utility preferences, the conditional heteroskedasticity generated by the higher-order terms is small; with Epstein-Zin preferences, it is appreciably larger. Although our affine solution ignores higher-order terms, conditional heteroskedasticity arises due to the presence of SV, and, indeed, our estimated DSGE model displays substantial time variation in the model-implied equity risk premium.

References

Ai, H. (2010). Information Quality and Long-Run Risk: Asset Pricing Implications. *Journal of Finance* 65:4, 1333–1367.

Ai, H., M. M. Croce, and K. Li (2013). Toward a Quantitative General Equilibrium Asset Pricing Model with Intangible Capital. *Review of Financial Studies* 26:2, 491–530.

Albuquerque, R., M. Eichenbaum, V. X. Luo, and S. Rebelo (2016). Valuation Risk and Asset Pricing. *Journal of Finance* 71:6, 2861–2903.

Andreasen, M. M. (2010). Stochastic Volatility and DSGE Models. *Economics Letters* 108:1, 7–9.

Andreasen, M. M. (2012). On the Effects of Rare Disasters and Uncertainty Shocks for Risk Premia in Non-Linear DSGE Models. *Review of Economic Dynamics* 15:3, 195–316.

Bansal, R., D. Kiku, I. Shaliastovich, and A. Yaron (2014). Volatility, the Macroeconomy, and Asset Prices. *Journal of Finance* 69:6, 2471–2511.

Bansal, R., D. Kiku, and A. Yaron (2012). An Empirical Evaluation of the Long-Run Risks Model for Asset Prices. *Critical Finance Review* 1:1, 183–221.

Bansal, R., D. Kiku, and A. Yaron (2016). Risks for the Long Run: Estimation with Time Aggregation. *Journal of Monetary Economics* 82:1, 52–69.

Bansal, R. and I. Shaliastovich (2013). A Long-Run Risks Explanation of Predictability Puzzles in Bond and Currency Markets. *Review of Financial Studies* 26:1, 1–33.

Bansal, R. and A. Yaron (2004). Risks for the Long Run: A Potential Resolution of Asset Pricing Puzzles. *Journal of Finance* 59:4, 1481–1509.

Basu, S. and B. Bundick (2017). Uncertainty Shocks in a Model of Effective Demand. *Econometrica* 85:3, 937–958.

Beeler, J. and J. Y. Campbell (2012). The Long-Run Risks Model and Aggregate Asset Prices: An Empirical Assessment. *Critical Finance Review* 1:1, 141–182.

Benigno, G., P. Benigno, and S. Nisticò (2013). Second-Order Approximation of Dynamic Models with Time-Varying Risk. *Journal of Economic Dynamics and Control* 37:7, 1231–1247.

Benninga, S. and A. Protopapadakis (1990). Leverage, Time Preference, and the 'Equity Premium Puzzle'. *Journal of Monetary Economics* 25:1, 49–58.

Bianchi, F., H. Kung, and M. Tirskikh (2019). The Origins and Effects of Macroeconomic Uncertainty. Manuscript.

van Binsbergen, J. H., J. Fernández-Villaverde, R. S. Koijen, and J. F. Rubio-Ramírez (2012). The Term Structure of Interest Rates in a DSGE Model with Recursive Preferences. *Journal of Monetary Economics* 59:7, 634–648.

Bloom, N. (2009). The Impact of Uncertainty Shocks. *Econometrica* 77:3, 623–685.

Boldrin, M., L. J. Christiano, and J. M. Fisher (2001). Habit Persistence, Asset Returns, and the Business Cycle. *American Economic Review* 91:1, 149–166.

Born, B. and J. Pfeifer (2014). Policy Risk and the Business Cycle. *Journal of Monetary Economics* 68:1, 68–85.

Caldara, D., J. Fernández-Villaverde, J. F. Rubio-Ramírez, and W. Yao (2012). Computing DSGE Models with Recursive Preferences and Stochastic Volatility. *Journal of Economic Dynamics and Contral* 15:2, 188–206.

Chen, A. Y. (2017). External Habit in a Production Economy: A Model of Asset Prices and Consumption Volatility Risk. *Review of Financial Studies* 30:8, 2890–2932.

Chen, Z. (2016). Time-to-Produce, Inventory, and Asset Prices. *Journal of Financial Economics* 120:2, 330–345.

Chib, S. and E. Greenberg (1994). Bayes Inference in Regression Models with ARMA(p, q) Errors. *Journal of Econometrics* 64:1–2, 183–206.

Chib, S. and E. Greenberg (1995). Understanding the Metropolis-Hastings Algorithm. *The American Statistician* 49:4, 327–335.

Chib, S. and S. Ramamurthy (2010). Tailored Randomized Block MCMC Methods with Applications to DSGE Models. *Journal of Econometrics* 155:1, 19–38.

Christiano, L. J., M. Eichenbaum, and S. Rebelo (2011). When is the Government Spending Multiplier Large? *Journal of Political Economy* 119:1, 78–121.

Cooper, I. and R. Priestly (2009). Time-Varying Risk Premiums and the Output Gap. *Review of Financial Studies* 22:7, 2801–2833.

Croce, M. M. (2014). Long-Run Productivity Risk: A New Hope for Production-Based Asset Pricing? *Journal of Monetary Economics* 66:1, 13–31.

Croce, M. M., T. T. Nguyen, S. Raymnond, and L. Schmid (2019). Government Debt and the Returns to Innovation. *Journal of Financial Economics* 132:3, 205–225.

de Groot, O. (2015). Solving Asset Pricing Models with Stochastic Volatility. *Journal of Economic Dynamics and Control* 52:1, 308–321.

de Groot, O. (2016). What Order? Perturbation Methods for Stochastic Volatility Asset Pricing and Business Cycle Models. Manuscript.

de Groot, O., A. W. Richter, and N. A. Throckmorton (2018). Uncertainty Shocks in a Model of Effective Demand: Comment. *Econometrica* 86:4, 1513–1526.

Del Negro, M., F. Schorfheide, F. Smets, and R. Wouters (2007). On the Fit of New Keynesian Models. *Journal of Business and Economic Statistics* 25:2, 123–143.

Dew-Becker, I. (2012). Essentially Affine Approximations for Economic Models. Manuscript.

Dew-Becker, I. (2014). Bond Pricing with a Time-Varying Price of Risk in an Estimated Medium-Scale Bayesian DSGE Model. *Journal of Money, Credit, and Banking* 46:5, 837–888.

Diebold, F. X., F. Schorfheide, and M. Shin (2017). Real-Time Forecast Evaluation of DSGE Models with Stochastic Volatility. *Journal of Econometrics* 201:2, 322–332.

Epstein, L. G. and S. E. Zin (1989). Substitution, Risk Aversion, and the Temporal Behavior of Consumption and Asset Returns: A Theoretical Framework. *Econometrica* 57:4, 937–969.

Epstein, L. G. and S. E. Zin (1991). Substitution, Risk Aversion, and the Temporal Behavior of Consumption and Asset Returns: An Empirical Analysis. *Journal of Political Economy* 99:2, 263–286.

Fama, E. F. and K. R. French (1989). Business Conditions and Expected Returns on Stocks and Bonds. *Journal of Financial Economics* 25:1, 23–49.

Faust, J. and A. Gupta (2012). Posterior Predictive Analysis for Evaluating DSGE Models. NBER Working Paper No. 17906.

Favilukis, J. and X. Lin (2016). Wage Rigidity: A Quantitative Solution to Several Asset Pricing Puzzles. *Revew of Financial Studies* 29:1, 148–192.

Fernández-Villaverde, J., P. A. Guerrón-Quintana, K. Kuester, and J. F. Rubio-Ramírez (2015a). Fiscal Volatility Shocks and Economic Activity. *American Economic Review* 105:11, 3352–3384.

Fernández-Villaverde, J., P. A. Guerrón-Quintana, and J. F. Rubio-Ramírez (2015b). Estimating Dynamic Equilibrium Models with Stochastic Volatility. *Journal of Econometrics* 185:11, 216–229.

Fernández-Villaverde, J., P. A. Guerrón-Quintana, J. F. Rubio-Ramírez, and M. Uribe (2011). Risk Matters: The Real Effects of Volatility Shocks. *American Economic Review* 101:6, 2530–2561.

Fernández-Villaverde, J. and J. F. Rubio-Ramírez (2007). Estimating Macroeconomic Models: A Likelihood Approach. *Review of Economic Studies* 74:4, 1059–1087.

Geweke, J. F. (2010). *Complete and Incomplete Econometric Models*. Princeton, NJ: Princeton University Press.

Gordon, R. J. (2016). *The Rise and Fall of American Growth*. Princeton, NJ: Princeton University Press.

Gourio, F. (2012). Disaster Risk and Business Cycles. *American Economic Review* 102:6, 2734–2766.

Greenwood, J., Z. Hercowitz, and G. W. Huffman (1988). Investment, Capacity Utilization, and the Real Business Cycle. *American Economic Review* 78:3, 402–417.

Guerrón-Quintana, P. A. (2010). What You Match Does Matter: The Effects of Data on DSGE Estimation. *Journal of Applied Econometrics* 25:5, 774–804.

Guvenen, F. (2009). A Parsimonious Macroeconomic Model for Asset Pricing. *Econometrica* 77:6, 1711–1750.

Hasseltoft, H. (2012). Stocks, Bonds, and Long-Run Consumption Risks. *Journal of Financial and Quantitative Analysis* 47:2, 309–332.

Hayashi, F. (1982). Tobin's Marginal q and Average q: A Neoclassical Interpretation. *Econometrica* 50:1, 213–224.

Hirshleifer, D., J. Li, and J. Yu (2015). Asset Pricing in Production Economies with Extrapolative Expectations. *Journal of Monetary Economics* 76:1, 87–106.

Jermann, U. J. (1998). Asset Pricing in Production Economies. *Journal of Monetary Economics* 41:2, 257–275.

Justiniano, A. and G. E. Primiceri (2008). The Time-Varying Volatility of Macroeconomic Fluctuations. *American Economic Review* 98:3, 604–641.

Justiniano, A., G. E. Primiceri, and A. Tambalotti (2010). Investment Shocks and Business Cycles. *Journal of Monetary Economics* 57:2, 132–145.

Justiniano, A., G. E. Primiceri, and A. Tambalotti (2011). Investment Shocks and the Relative Price of Investment. *Review of Economic Dynamics* 14:1, 102–121.

Kaltenbrunner, G. and L. A. Lochstoer (2010). Long-Run Risk Through Consumption Smoothing. *Review of Financial Studies* 23:8, 3190–3224.

Kilic, M. and J. A. Wachter (2018). Risk, Unemployment, and the Stock Market: A Rare-Event-Based Explanation of Labor Market Volatility. *Review of Financial Studies* 31:12, 4762–4814.

Kim, S., N. Shephard, and S. Chib (1998). Stochastic Volatility: Likelihood Inference and Comparison with ARCH Models. *Review of Economic Studies* 65:3, 361–393.

Kung, H. (2015). Macroeconomic Linkages Between Monetary Policy and the Term Structure of Interest Rates. *Journal of Financial Economics* 115:1, 42–57.

Lettau, M. (2003). Inspecting the Mechanism: Closed-Form Solutions for Asset Prices in Real Business Cycle Models. *Economic Journal* 113:489, 550–575.

Lettau, M. and H. Uhlig (2000). Can Habit Formation Be Reconciled with Business Cycle Facts? *Review of Economic Dynamics* 3:1, 79–99.

Li, E. X. N. and F. Palomino (2014). Nominal Rigidities, Asset Returns, and Monetary Policy. *Journal of Monetary Economics* 66:1, 210–225.

Liu, Z., D. F. Waggoner, and T. Zha (2011). Sources of Macroeconomic Fluctuations: A Regime-Switching DSGE Approach. *Quantitative Economics* 2:2, 251–301.

Malkhozov, A. (2014). Asset Prices in Affine Real Business Cycle Models. *Journal of Economic Dynamics and Control* 45:1, 180–193.

Mehra, R. and E. C. Prescott (1985). The Equity Premium: A Puzzle. *Journal of Monetary Economics* 15:2, 145–161.

Nakamura, E., D. Sergeyev, and J. Steinsson (2017). Growth-Rate and Uncertainty Shocks in Consumption: Cross-Country Evidence. *American Economic Journal: Macroeconomics* 9:1, 1–39.

Pohl, W., K. Schmedders, and O. Wilms (2018). Higher Order Effects in Asset Pricing Models with Long-Run Risks. *Journal of Finance* 73:3, 1061–1111.

Rapach, D. E., J. K. Strauss, and G. Zhou (2010). Out-of-Sample Equity Premium Prediction: Combination Forecasts and Links to the Real Economy. *Review of Financial Studies* 23:2, 821–862.

Restoy, F. and G. M. Rockinger (1994). On Stock Market Returns and Returns on Investment. *Journal of Finance* 49:2, 543–556.

Rouwenhorst, K. G. (1995). Asset Pricing Implications of Equilibrium Business Cycle Models. In *Frontiers of Business Cycle Research*. Ed. by T. F. Cooley. Princeton, NJ: Princeton University Press, pp. 294–330.

Rudebusch, G. D. and E. T. Swanson (2012). The Bond Premium in a DSGE Model with Long-Run Real and Nominal Risks. *American Economic Journal: Macroeconomics* 4:1, 105–143.

Schmitt-Grohé, S. and M. Uribe (2004). Solving Dynamic General Equilibrium Models Using a Second-Order Approximation to the Policy Function. *Journal of Economic Dynamics and Control* 28:4, 755–775.

Sims, C. A. (2002). Solving Linear Rational Expectations Models. *Computational Economics* 20:1–2, 1–20.

Smets, F. and R. Wouters (2003). An Estimated Dynamic Stochastic General Equilibrium Model of the Euro Area. *Journal of the European Economic Association* 1:5, 1123–1175.

Stock, J. H. and M. W. Watson (2002). Has the Business Cycle Changed and Why? In *NBER Macroeconomics Annual 2002*. Ed. by M. Gertler and K. Rogoff. Cambridge, MA: MIT Press, pp. 159–218.

Tallarini, T. D. (2000). Risk-Sensitive Real Business Cycles. *Journal of Monetary Economics* 45:3, 507–532.

Tanner, M. A. and W. H. Wong (1987). The Calculation of Posterior Distributions by Data Augmentation. *Journal of the American Statistical Association* 82:398, 528–540.

Weil, P. (1989). The Equity Premium Puzzle and the Risk-Free Rate Puzzle. *Journal of Monetary Economics* 24:3, 401–421.

Table 1: Summary statistics for observable variables, 1973:1–2018:4

(1) Variable	(2) Mean (%)	(3) Volatility (%)	(4) Minimum (%)	(5) Maximum (%)	(6) Auto-correlation
Log equity market excess return	1.23	8.25	−30.89	19.30	0.09
Ex ante log real risk-free return	0.34	0.57	−0.59	1.72	0.94
Real consumption log growth	0.52	0.49	−2.30	1.63	0.44
Real investment log growth	0.38	2.87	−10.72	7.35	0.41
Real compensation log growth	0.38	0.80	−4.19	2.48	0.35

The table reports summary statistics for the observable variables used for Bayesian estimation of the DSGE model. To compute the ex ante log real risk-free return, we first calculate the log real return for Treasury bills based on the Treasury bill total return index (from Global Financial Data) and gross domestic product deflator (from FRED). The proxy for the ex ante log real risk-free return is the projection of the log real return for Treasury bills on the nominal three-month US Treasury bill yield (from FRED) and inflation rate (computed from the gross domestic product deflator) over the previous four quarters. The log equity market excess return is the log real equity market return minus the ex ante log real risk-free return, where the real equity market return is computed from the S&P 500 total return index (from Global Financial Data) and gross domestic product deflator. Consumption is the sum of personal consumption expenditures on nondurables and services (from FRED). Investment is the sum of personal consumption expenditures on durables and gross domestic private investment (from FRED). Compensation is the compensation of employees out of gross domestic income (from FRED). Real consumption, investment, and compensation are computed using the gross domestic product deflator and converted to per capita terms using the total US population (from FRED).

Table 2: DSGE model estimation results

(1)	(2)	(3)	(4)	(5)	(6)	(7)
	Prior			Posterior		
Parameter	Type	Para(1)	Para(2)	Mean	90% credible probability interval	Inefficiency factor
ψ	Gamma	2.00	0.30	1.79	[1.30 , 2.27]	38.3
ϕ	Gamma	6.00	2.00	10.30	[7.53 , 12.83]	36.0
χ	Gamma	1.50	0.50	0.31	[0.25 , 0.37]	44.0
r^{Q}	Gamma	0.30	0.10	1.80	[1.57 , 2.04]	40.4
γ^{Q}	Gamma	0.40	0.10	0.43	[0.32 , 0.54]	24.3
ρ_{υ}	Beta	0.80	0.05	0.995	[0.993 , 0.997]	23.5
ρ_{ν}	Beta	0.80	0.05	0.97	[0.95 , 0.98]	48.8
ρ_{z}	Beta	0.20	0.10	0.12	[0.05 , 0.18]	44.0
φ_{υ}	Gamma	1.00	0.50	0.05	[0.04 , 0.06]	62.6
φ_{ν}	Gamma	1.00	0.50	4.75	[3.86 , 5.49]	49.8
$\sigma \times 10^2$	IG-1	4.00	0.40	2.04	[1.82 , 2.27]	49.8
ρ_{σ}	Beta	0.80	0.05	0.84	[0.80 , 0.88]	20.8
$\varphi_{\sigma} \times 10^4$	IG-1	4.00	0.05	0.06	[0.03 , 0.08]	55.7
ϑ	Gamma	1.50	0.10	1.78	[1.64 , 1.93]	25.7

The table reports Bayesian estimates of the DSGE model parameters. The parameters r^{Q} and γ^{Q} are related to β and γ by $\beta = 1/\left[\left(r^{\mathrm{Q}}/100\right) + 1\right]$ and $\gamma = 1 + \left(\gamma^{\mathrm{Q}}/100\right)$, respectively. Two parameters are fixed ($\alpha = 0.36$ and $\delta = 0.025$). The estimation sample period is 1973:1 to 2018:4. IG-1 is the Inverse-Gamma Type 1 distribution. Para(1) and Para(2) correspond to the mean and standard deviation, respectively, for the Gamma and Beta distributions; Para(1) and Para(2) correspond to ν and s, respectively, for the IG-1 distribution, where $p(\sigma) \propto \sigma^{-\nu-1} e^{-\frac{\nu s^2}{2\sigma^2}}$. The estimates are based on 10,000 draws (after 5,000 burn-in draws) generated by the Markov chain Monte Carlo algorithm. The inefficiency factor is computed as $1 + 2\sum_{k=1}^{K} w(k/K)\rho(k)$, where $K = 200$, $\rho(k)$ is the autocorrelation at lag k for the sequence of parameter draws, and $w(\cdot)$ is the Parzen kernel.

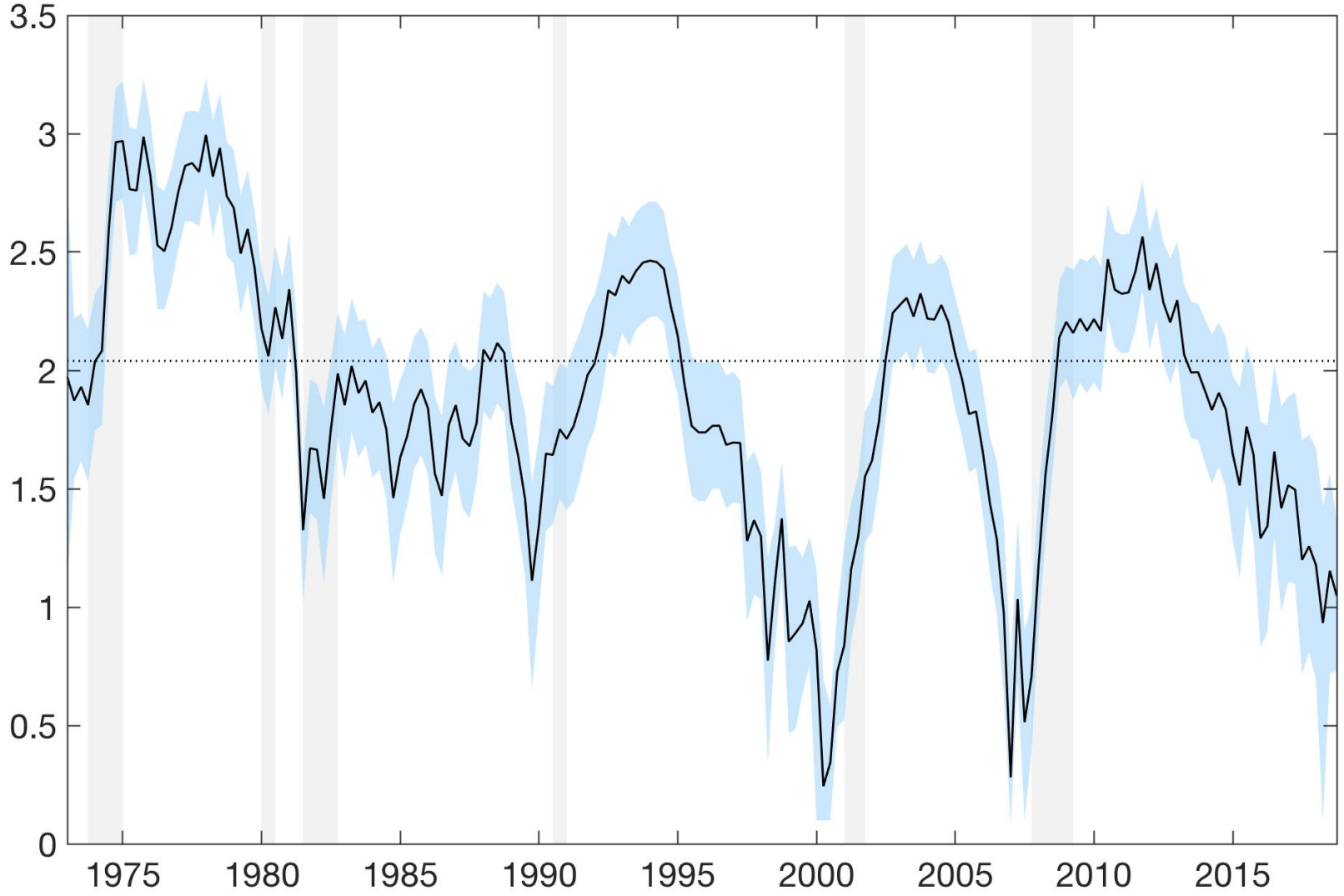

Figure 1: Common stochastic volatility component, 1973:1–2018:4

The figure depicts the posterior estimate of σ_t (in percent) for the DSGE model. The solid line is the posterior mean. Bands delineate posterior 90% credible probability intervals. The dotted horizontal line is the posterior mean for σ. Vertical bars delineate recessions as dated by the National Bureau of Economic Research.

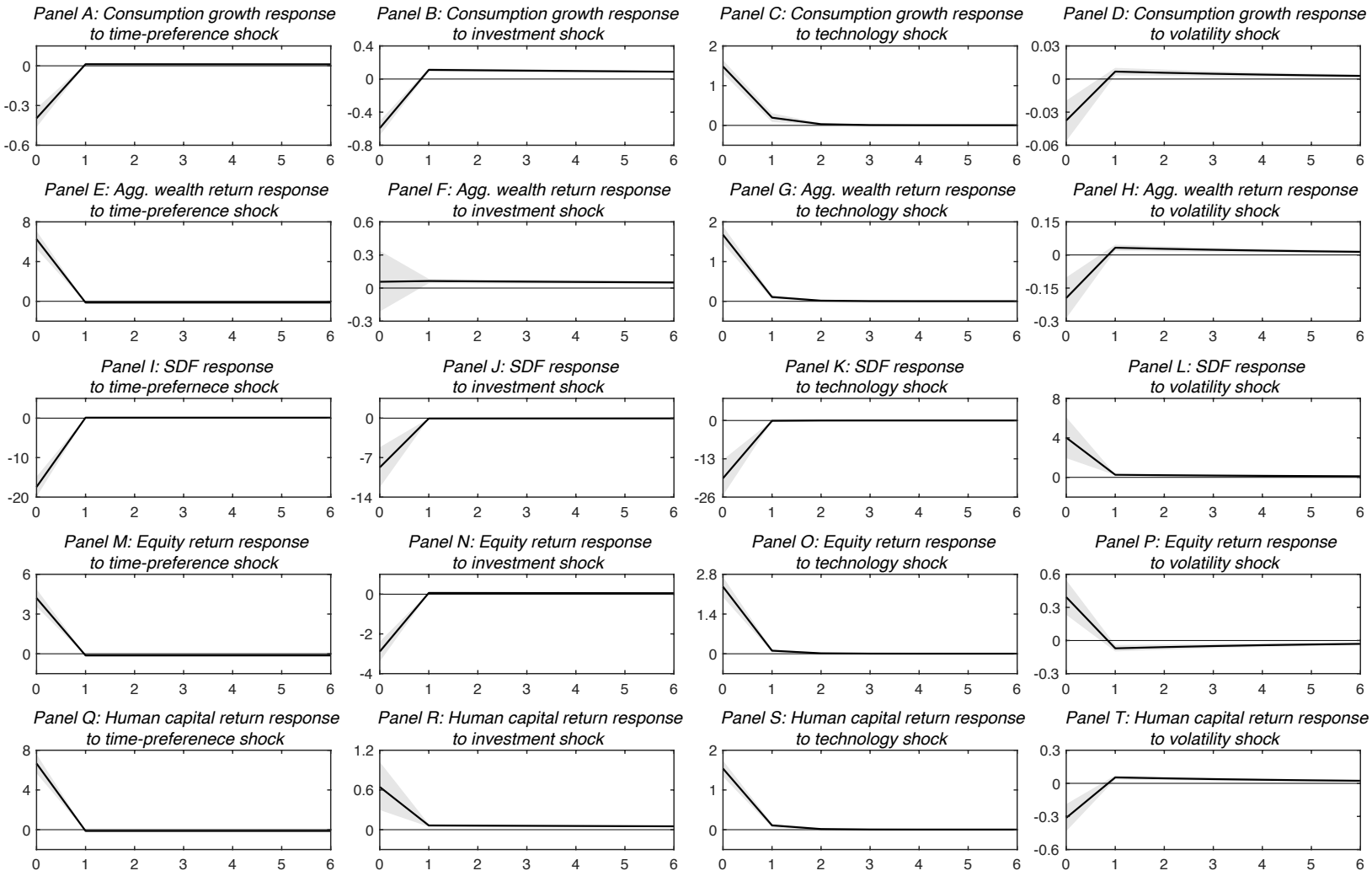

Figure 2: Responses to structural shocks

Each panel depicts the response to a one-standard-deviation innovation to a structural shock for the variable-shock pair given in the panel heading. The variables are in logs multiplied by 100. The solid line is the posterior mean. Bands delineate posterior 90% credible probability intervals. The horizontal axis gives the number of periods after the shock.

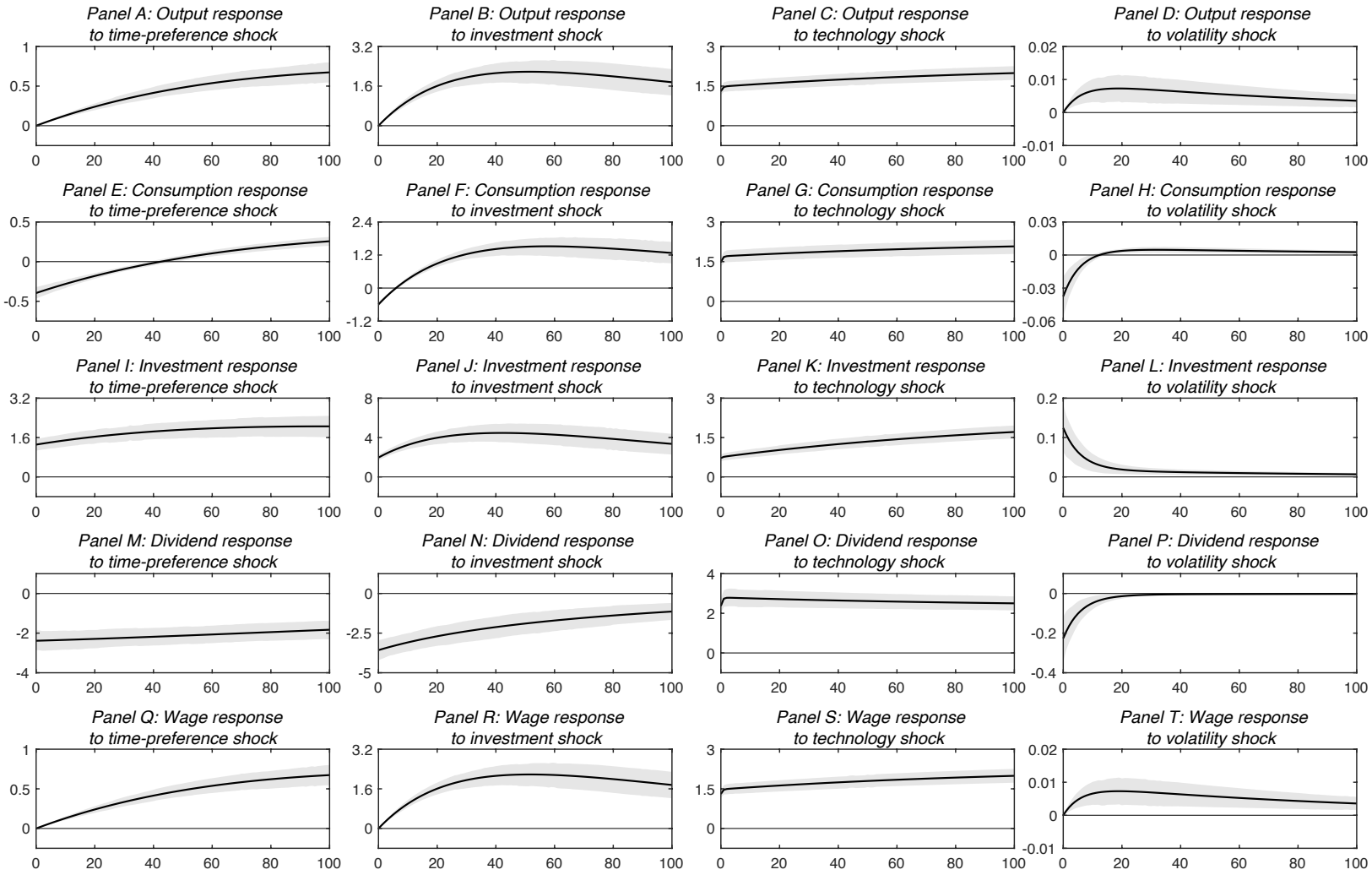

Figure 3: Macroeconomic variable responses to structural shocks

Each panel depicts the response to a one-standard-deviation innovation to a structural shock for the variable-shock pair given in the panel heading. The variables are in logs multiplied by 100. The solid line is the posterior mean. Bands delineate posterior 90% credible probability intervals. The horizontal axis gives the number of periods after the shock.

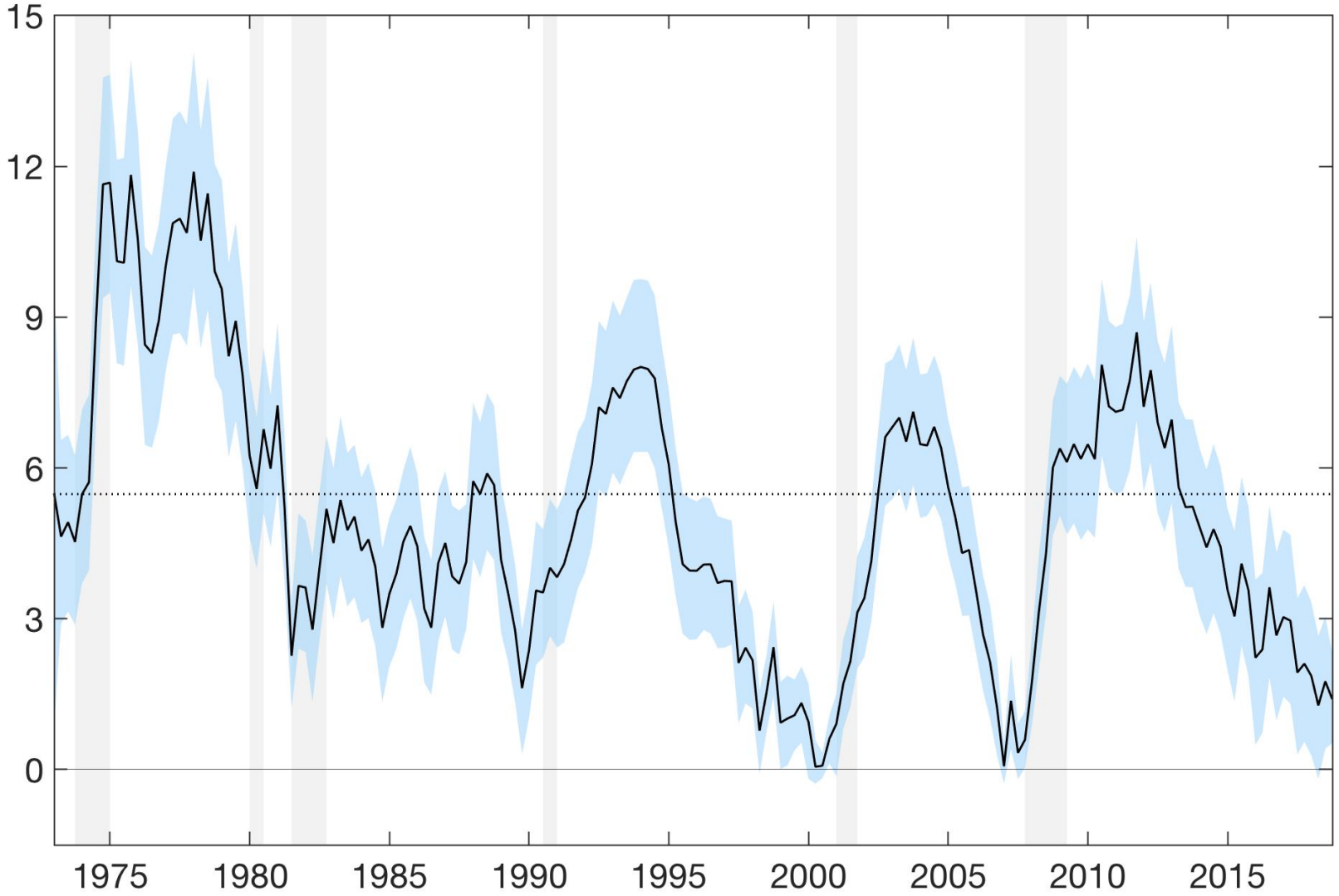

Figure 4: Annualized log equity risk premium, 1973:1–2018:4

The figure depicts the posterior estimate of the annualized time-varying log equity risk premium (in percent) for the DSGE model. The solid line is the posterior mean. Bands delineate posterior 90% credible probability intervals. The dotted horizontal line is the posterior mean for the steady-state log equity risk premium. Vertical bars delineate recessions as dated by the National Bureau of Economic Research.